Effect of Urea on Human Serum Albumin

And

Its Complex With Warfarin

Chapter 1

Introduction

INTRODUCTION

Human serum albumin (HSA), the most abundant protein in human plasma, accounts for about 60% of the total serum proteins (Carter and Ho, 1994). It is also distributed to the interstitial fluid of the body tissues. HSA is synthesized in the liver, and exported to other parts as a non-glycosylated protein. The protein binds to a number of relatively insoluble endogenous compounds such as unesterified fatty acids, bilirubin, bile acids etc and thus makes their transport easier throughout the circulation (Kragh-Hansen, 1990; Peters, 1995). It also has the ability to bind a broad spectrum of drugs, and much of the importance of this protein has been referred to as its effects on drug delivery. Drug binding to HSA plays an important role in the pharmacokinetics of the drug by limiting the unbound concentration and affecting its administration and elimination (Carter and Ho, 1994; Peters, 1995). In some cases, the major fraction of the administered drug is determined by HSA. For example, warfarin [3-(∝-acetonylbenzyl)-4-hydroxycoumarin], a widely used anticoagulant drug for the treatment of venous thrombosis and pulmonary embolism (Bell and Simon, 1982; Petersen *et al.,* 1989; Petersen and Kwaan, 1986), as well as in the prevention of prosthetic heart valve thromboembolism (Mok *et al.,* 1985), which is 99% bound to the protein (HSA) under normal therapeutic conditions and is therefore known as a drug with small volume of distribution and low clearance (Holford and Benet, 1998).

HSA is comprised of a single polypeptide chain with 585 amino acid residues, arranged in three structurally similar ∝-helical domains, namely, domains I, II and III. Each domain is further divided into two subdomains, A and B, which include

six and four ∝-helices, respectively connected by long ∝-helical chains involving residues: 101-124, 289-316 and 487-514. These domains are connected with each other through nonhelical segments between 177-200 and 369-392 residues (Carter *et al.,* 1989; Carter and He, 1990).

Interactions of pharmaceutical drugs with serum components play an important role in drug delivery. Specific interactions of drugs and their competition for binding sites on transport proteins can significantly influence their distribution in serum. HSA, being the major transport protein of mammalian blood circulation binds a large number of drugs varying in structure. Therefore, information on the drug-HSA interaction will give a better understanding of the absorption and distribution of a particular drug. Structural studies have shown specific locations of the drug binding sites on HSA involving some domains or subdomains of the protein (He and Carter, 1992). Thus, many drugs bind to one of the two primary binding sites on the protein, known as Sudlow's sites I and II (Sudlow *et al.,* 1975).

Warfarin is known to bind to site I of HSA, which is also known as the warfarin-azapropazone binding site (Birkett *et al.,* 1980; Fehske *et al.,* 1981; Fehske *et al.,* 1982). This site is composed of overlapping regions and is responsible for the specific binding of warfarin and other drugs such as azapropazone and phenylbutazone. Due to its well-characterized interaction to HSA, warfarin is often used as a marker ligand for the specific binding to site I on HSA (Sjoholm *et al.,* 1979). In other words, warfarin is being employed as a probe to study the interactions of other drugs at Sudlow site I on HSA (Oida, 1986; Bertucci *et al.,*

1999). The warfarin binding site is a hydrophobic cavity in subdomain IIA, formed as a result of packing of all six helices of subdomain IIA (He and Carter, 1992). Warfarin binding to HSA involves both hydrophobic (dominant) and electrostatic interactions. Several hydrophobic residues (Phe-211, Trp-214, Leu-219, Leu-238, Val-241, Ile-260, Ile-264, Ile-280 and Ala-291) as well as aliphatic portions of some polar residues (Arg-218, Arg-222, His-242, Arg-257 and Ser-287) in the binding pocket offer hydrophobic contacts to the incoming ligand (warfarin). On the other hand, Arg-222 and His-242 contribute to electrostatic interactions between warfarin and HSA (Petitpas *et al.,* 2001).

Formation of native, globular and biologically active conformation of a protein is the result of protein folding involving both noncovalent and covalent interactions. Importance of the globular conformation of a protein for its biological function can be reflected by the complete loss of biological activity in presence of denaturants (Tanford, 1968). Denaturation usually results in the destruction of the protein's tertiary structure, leading to the change in its ligand binding ability since all functions of proteins are displayed by their three-dimensional structures (Dill and Shortle, 1991). Alteration in protein's binding ability due to unfolding process as seen in patients with renal or liver disease (Kremer *et al.,* 1988) as well as elderly patients (Leslie *et al.,* 1992) can be reflected by the unbound drug concentration in plasma. Urea and guanidine hydrochloride are the two common chemical denaturants employed for protein denaturation studies. These denaturants bind to the peptide groups and weaken internal hydrogen bonds in

proteins, and change the surrounding water structure, thus weaken the hydrophobic interactions as well (De Aspuru and Zaton, 1993).

The purpose of this study was to examine the effect of urea on the three-dimensional structure of HSA as well as on its interaction with warfarin in order to correlate the change in drug binding with the protein conformation. In other words, we studied the binding of warfarin to both native and altered conformations of HSA induced by different urea concentrations using fluorescence spectroscopic method due to its great sensitivity.

Chapter 2

Literature review

LITERATURE REVIEW

2.1 GENERAL

Serum albumin is the most abundant soluble protein constituent of blood plasma with a typical concentration of 50g/L (Carter and Ho, 1994). It has been categorized as a member of the multigene protein family that includes other plasma proteins such as ∝-fetoprotein (AFP) (Deutsh, 1991) and the human group specific component (Gc) or vitamin D-binding protein (Cooke and Hadded, 1989). The name 'albumin' evolved from a German word for protein, *albumen.* Originally, it was derived from the Latin word; *albus* meaning white, based on the colour of the part surrounding the yolk of a cooked egg. Furthermore, the ending '*–in'* specified a protein from blood plasma. Under normal conditions, albumin concentration remains usually very low in other parts of the body in comparison to the plasma (Halliwell, 1988). Thus, around 40% of total albumin is present in the circulatory plasma (Peters, 1992) while half of the remaining 60% in viscera and half in skin and muscle (Rabilloud *et al.,* 1988). Albumin has also been identified in amniotic fluid (Bala *et al.,* 1987), semen (Blumsohn *et al.,* 1991), milk (Phillippy and McCarthy, 1979) and mammary cysts (Balbin *et al.,* 1991). The normal concentration of albumin in human plasma varies between 35 and 50g/L through transcriptional control of the albumin gene by the anabolic hormones, insulin and somatotropin (Hutson *et al.,* 1987; Peters, 1996). Albumin plays an important role in the circulatory system for transporting a large number of endogenous and exogenous compounds such as drugs, metabolites, fatty acids

and metal ions as well as in the regulation of osmotic pressure and fluid distribution among various parts of the body (Carter and Ho, 1994).

It is one of the few proteins commercially available with high purity and low cost. These properties in addition to its solubility and lack of prosthetic groups/ carbohydrates have made it as the best choice for a model protein in different fields including research. Many studies on albumin have been reported in the literature, giving details of its different properties including its biological and physiological aspects, chemistry, structure, metabolism, genetics and clinical applications, etc (Foster, 1960; Rosenoer *et al.,* 1977; Peters, 1985). A book entitled "All about Albumin. Biochemistry, Genetics and Medical Application" has also been written by Peters (1996) and published by Academic Press Inc., New York.

2.2 PHYSICO-CHEMICAL PROPERTIES OF HSA

Most of the studies have been performed using albumin purified from bovineor human plasma. Table 2.1 summarizes some of the physico-chemical properties of human serum albumin (HSA). A value of 66,438Da has been assigned for molecular mass of HSA based on its amino acid composition (Minghetti *et al.,* 1986). Values of sedimentation coefficient ($S^o_{20,w}$), diffusion coefficient ($D^o_{20,w}$) and partial specific volume ($\bar{v}_2$) of HSA were measured as 4.6×10^{-13}s, $6.1\times 10^{-7} cm^2$/sec and 0.733cc/g respectively (Oncley *et al.,* 1947; Hunter, 1966). The intrinsic viscosity [η] and frictional coefficient (f/f_o) for the protein were found as 4.2cc/g (Hunter, 1966) and 1.28 (Oncley *et al.,* 1947) respectively. HSA was

found to possess an overall dimensions of 38×150Å (Hughes, 1954) with an axial ratio of around 3.9:1 (Oncley *et al.*, 1947). It has an isoelectric point of 4.7 (Longsworth and Jacobsen, 1949) whereas the isoionic point was 5.16 (Hughes, 1954). HSA contains about 67% α-helix and 10% β-form as reported by Carter and Ho (1994). The specific extinction coefficient, $E_{1cm}^{1\%}$ of HSA at 279nm was determined as 5.31 (Janatova *et al.*, 1968).

2.3 STRUCTURE OF HSA

2.3.1 Amino acid composition

HSA is known as a simple protein due to the presence of amino acids only and lack of any other groups such as carbohydrate or any other non-protein moiety. Table 2.2 shows the amino acid composition of HSA. Albumin is characterized by the low content of isoleucine, methionine and glycine residues, whereas it has high content of leucine, cysteine and charged amino acids such as aspartic acid, glutamic acid, lysine and arginine. It is also characterized by the presence of a single tryptophan (Trp) residue (Minghetti *et al.,* 1986). Out of 35 cysteine (Cys) residues, 34 Cys are involved in the formation of 17 disulfide bonds, leaving only one Cys residue free. The high content of ionized residues in albumin (about 185 ions per molecule at pH 7.0) makes it a molecule with a high total charge leading to its greater solubility.

2.3.2 Primary structure

HSA contains 585 amino acid residues, arranged in the form of a linear sequence in a single polypeptide chain (Brown, 1976; Carter and Ho, 1994). Figure 2.1

Table 2.1 Some physico-chemical properties of human serum albumin.

Property	**Value**	**Reference**
Molecular mass (*From amino acid composition*)	66,438Da	Minghetti *et al.* (1986)
Sedimentation coefficient, $S^o_{20,w}$	4.6×10^{-13}s	Oncley *et al.* (1947)
Diffusion coefficient, $D^o_{20,w}$	6.1×10^{-7}dcm^2/s	" "
Frictional coefficient, f/f_o	1.28	" "
Partial specific volume, $\bar{v}_2$	$0.733cm^3$/g	Hunter (1966)
Intrinsic viscosity, [η]	4.2cc/g	" "
Overall dimensions	38×150 Å	Hughes (1954)
Axial ratio	3.9:1	Oncley *et al.* (1947)
Isoelectric point	4.7	Longsworth and Jacobsen (1949)
Isoionic point	5.16	Hughes (1954)
$E^{1\%}_{1cm}$ at 279nm	5.31	Janatova *et al.* (1968)
Secondary structures		
α-helix, %	67	Carter and Ho (1994)
β-form, %	10	Carter and Ho (1994)

shows the loop-link-loop pattern in the primary structure of HSA, whereas the amino acid sequence of HSA, as derived from the cDNA data, is given in Figure 2.2. Primary structure of HSA is very close to bovine serum albumin (BSA) in its disulfide bonding pattern and has 76% sequence homology (Peters, 1985; He and Carter, 1992; Carter and Ho, 1994). In all known albumin sequences, about 50% of residues are conserved (Carter and Ho, 1994). The 17 disulphide bridges of HSA create nine double loops (L1−L9) producing a pattern of three α-helical domains, namely, I, II and III as shown in Figure 2.1 (He and Carter, 1992). All loops do not have same length, but they are arranged in a triplet fashion of a long-short-long pattern to make three homologous domains.

Each domain consists of two longer loops, separated by a shorter loop. Domains I, II and III are comprised of residues 1−195, 196−383 and 384−585 respectively in the primary sequence of HSA (Carter and Ho, 1994). The average sequence homology among these domains is around 18−25%, being 25%, 21% and 18% between domains I and II, II and III and I and III respectively (Brown, 1977). At neutral pH, the negative charge distribution in across the surface of the HSA molecule is -9, -8 and $+2$ for domains I, II and III respectively (Peters, 1996). The conformation of disulfide bridges exhibits both gauche-gauche-gauche and gauche-gauche-trans conformations and their conformations are changed during acid-induced isomerization (Nakamura *et al.,* 1997).

Table 2.2 Amino acid composition of human serum albumin.*

Amino acid	Three-letter abbreviation	One-letter symbol	Number of residues
Glycine	Gly	G	12
Alanine	Ala	A	62
Valine	Val	V	41
Leucine	Leu	L	61
Isoleucine	Ile	I	8
Proline	Pro	P	24
Serine	Ser	S	24
Threonine	Thr	T	28
Aspartic acid	Asp	D	36
Asparagine	Asn	N	17
Glutamic acid	Glu	E	62
Glutamine	Gln	Q	20
Histidine	His	H	16
Lysine	Lys	K	59
Arginine	Arg	R	24
Phenylalanine	Phe	F	31
Tyrosine	Tyr	Y	18
Tryptophan	Trp	W	1
Cysteine	Cys	C	35
Methionine	Met	M	6
Total			585

* Taken from Minghetti *et al.* (1986)

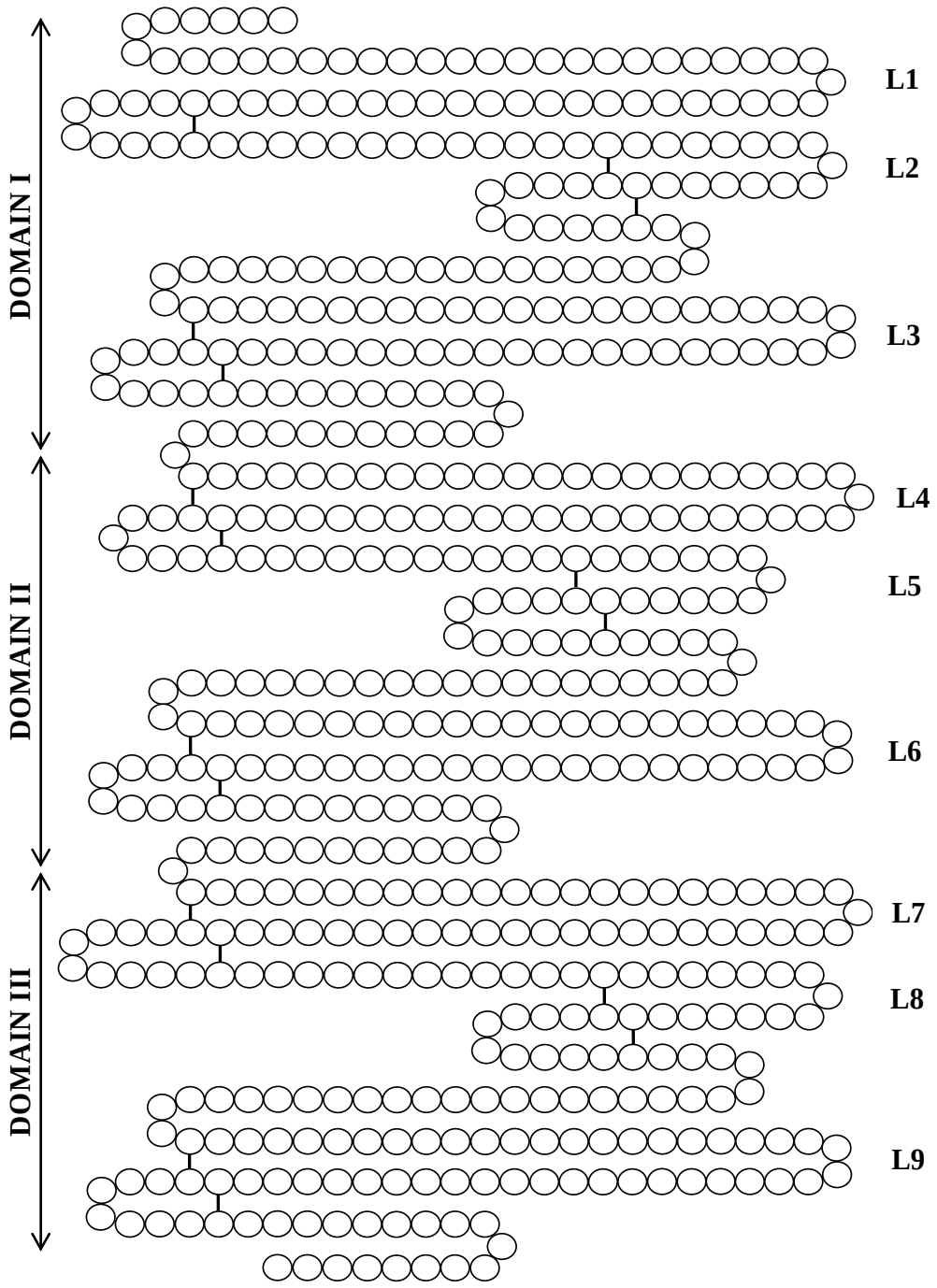

Figure 2.1 Illustration of the loop-link-loop pattern in the primary structure of serum albumin showing different domains and loops (L1-L9) (Taken from Carter and Ho, 1994).

1	10	20	30	40	50
DAHKSEVAHR	**FKDLGEENFK**	**ALVLIAFAQY**	**LQQCPFEDHV**	**KLVNEVTEFA**	
60	70	80	90	100	
KTCVADESAE	**NCDKSLHTLF**	**GDKLCTVATL**	**RETYGEMADC**	**CAKQEPERNE**	
110	120	130	140	150	
CFLQHKDDNP	**NLPRLVRPEV**	**DVMCTAFHDN**	**EETFLKKYLY**	**EIARRHPYFY**	
160	170	180	190	200	
APELLFFAKR	**YKAAFTECCQ**	**AADKAACLLP**	**KLDELRDEGK**	**ASSAKQRLKC**	
210	220	230	240	250	
ASLQKFGERA	**FKAWAVARLS**	**QRFPKAEFAE**	**VSKLVTDLTK**	**VHTECCHGDL**	
260	270	280	290	300	
LECADDRADL	**AKYICENQDS**	**ISSKLKECCE**	**KPLLEKSHCI**	**AEVENDEMPA**	
310	320	330	340	350	
DLPSLAADFV	**ESKDVCKNYA**	**EAKDVFLGMF**	**LYEYARRHPD**	**YSVVLLLRLA**	
360	370	380	390	400	
KTYETTLEKC	**CAAADPHECY**	**AKVFDEFKPL**	**VEEPQNLIKQ**	**NCELFKQLGE**	
410	420	430	440	450	
YKFQNALLVR	**YTKKVPQVST**	**PTLVEVSRNL**	**GKVGSKCCKH**	**PEAKRMPCAE**	
460	470	480	490	500	
DYLSVVLNQL	**CVLHEKTPVS**	**DRVTKCCTES**	**LVNRRPCFSA**	**LEVDETYVPK**	
510	520	530	540	550	
EFNAETFTFH	**ADICTLSEKE**	**RQIKKQTALV**	**ELVKHKPKAT**	**KEQLKAVMDD**	
560	570	580	585		
FAAFVEKCCK	**ADDKETCFAE**	**EGKKLVAASQ**	**AALGL**		

Figure 2.2 Amino acid sequence of human serum albumin (Taken from Minghetti *et al.,* 1986).

2.3.3 Three-dimensional structure

The analysis of the three-dimensional (3-D) structure of HSA using X-ray diffraction at 3.2 Å resolution shows the involvement of 67% of the total residues of crystalline HSA in 28 α-helical regions, whereas the rest of the chain is extended peptide chain with a 10% β turn (Carter and Ho, 1994). Figure 2.3 shows schematic drawing of a heart-shaped HSA molecule, consisting of three domains, which are made up of nine loops and 17 disulfide bridges (He and Carter, 1992). Each domain is further divided into two sub-domains, namely, A and B, which are widely cross-linked by the disulphide bridges. There are 10 principal helices for the two subdomains, h1−h6 for sub-domain A and h7−h10 for sub-domain B. The connections between domains I−II and II−III in turn are made through h10(I)−h1(II) and h10(II)−h1(III) extensions, respectively. Various loops, such as L1-L2, L4-L5 and L7-L8 are grouped as subdomains IA, IIA and IIIA, respectively whereas loops L3, L6 and L9 form subdomains IB, IIB and IIIB respectively. In HSA, the single Trp residue (Trp-214) is located in loop L4.

The stability of overall native 3-D conformation of HSA is maintained by various factors such as intra- and inter-domain forces like salt bridges, hydrophobic interactions and natural boundaries of helical extensions present between three domains. Two primary binding sites in HSA (Site I and II) are characterized by the hydrophobic cavities for the binding of various compounds and are located in subdomains IIA and IIIA respectively (He and Carter, 1992).

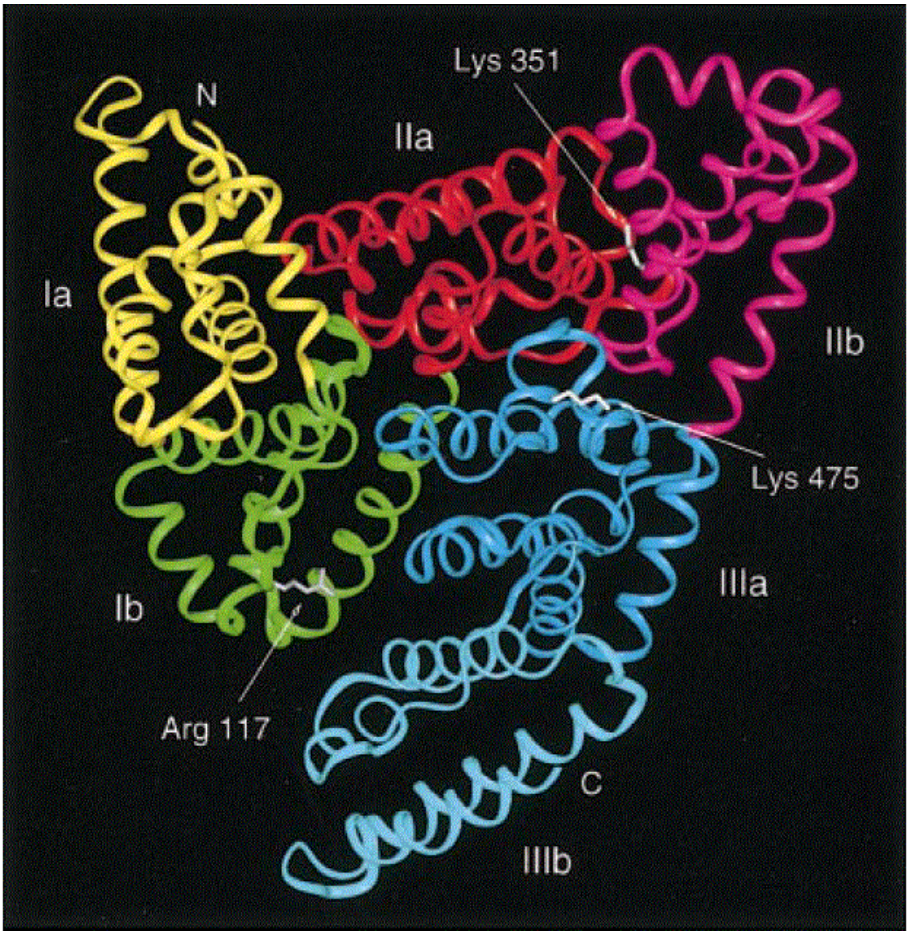

Figure 2.3 Schematic drawing of the HSA molecule. Each subdomain is marked with a different color (yellow for subdomain Ia; green, Ib; red, IIa; magenta, IIb; blue, IIIa and cyan, IIIb). N- and C-termini are marked as N and C, respectively (Taken from Sugio *et al.,* 1999).

2.4 DENATURATION

Due to the requirement of the native and globular conformation of a protein for its biological function, a number of denaturation studies have been performed on serum albumin to understand its folding mechanism. These studies involved the use of different denaturants such as temperature, pH, pressure and chemical denaturants like urea and guanidine hydrochloride (GdnHCl) (Hayakawa *et al.,* 1996; Tanaka *et al.,* 1997; Flora *et al.,* 1998; Kosa *et al.,* 1998; Farruggia and Pico, 1999; Muzammil *et al.,* 1999; 2000; Tayyab *et al.,* 2000; Gonzalez-Jimenez and Cortijo, 2002; Krishnakumar and Panda, 2002; Santra *et al.,* 2004; Ahmad *et al.,* 2005; Sen *et al.,* 2008; Rownicka-Zubik *et al.,* 2009). Denaturation of a protein usually results in the transformation of its tertiary structure into primary structure, which is capable of regaining native structure of the protein after removal of the denaturants by slow oxidation of its thiol groups to disulfide bonds (Anfinsen, 1973; Johanson *et al.,* 1977; Wichman *et al.,* 1977; Chavez and Benjamin, 1978).

Denaturation of serum albumin has been studied using different probes such as intrinsic fluorescence, circular dichroism (CD) spectral signal, 1-anilinonaphthalene-8-sulfonic acid (ANS) fluorescence, ultraviolet (UV) difference spectral signal, reduced viscosity etc (Khan *et al.,* 1987; Tayyab *et al.,* 1995; Pico, 1995; Farruggia *et al.,* 1997; Muzammil *et al.,* 2000; Gonzalez-Jimennez and Cortijo, 2002; Kumar *et al.,* 2005). In HSA, the presence of a single Cys residue in domain I, a single Trp residue in domain II and a number of reactive Tyr residues in domain III support the possibility to study the unfolding

and folding pathways of each domain (Brown, 1977; Means and Wu, 1979; Fehske *et al.,* 1980; Flora *et al.,* 1998; Krishnakumar and Panda, 2002). Both chemical denaturants (urea and GdnHCl) denature proteins through their binding to the peptide groups and weakening the internal hydrogen bonds of the protein as well as changing the surrounding water structure, thus weakening the hydrophobic interactions as well (De Aspuru and Zaton, 1993). Earlier studies on urea denaturation of HSA using intrinsic fluorescence measurements upon excitation at 280nm have shown a two-step, three-state transition with the presence of a stable intermediate around 4.8−5.2M urea whereas the transition displayed a single-step, two-state process when the urea denaturation was monitored by Trp fluorescence (Khan *et al.,* 1987; Ahmad and Qasim, 1995; Muzammil *et al.,* 2000; Tayyab *et al.,* 2000; 2002). Urea denaturation of serum albumin has been suggested to start with the unfolding of domain III followed by the unfolding of the remaining two domains (Tanaka *et al.,* 1993; Ahmad and Qasim, 1995). Various domain specific ligands such as drugs and non-drug ligands have been widely used to study urea denaturation of serum albumin (Tayyab *et al.,* 2000; Santra *et al.,* 2004; Rownicka-Zubik *et al.,* 2009). GdnHCl denaturation of serum albumin has shown a single-step, two-state transition (Farruggia and Pico, 1999; Kosa *et al.,* 1998; Kamal *et al.,* 2004).

2.5 LIGAND BINDING

The main function of HSA besides controlling the osmotic pressure, is the transport of a wide variety of endogenous and exogenous ligands, both anionic and cationic in nature (Figure 2.4). These include fatty acids, hormones,

metabolites, metal ions, amino acids, steroids, dyes, drugs etc (Hultmark *et al.,* 1975; Sollene *et al.,* 1981; Spector, 1986; Watanabe *et al.,* 1991; Sadler *et al.,* 1994; Peters, 1996). These ligands (both hydrophilic and hydrophobic in nature) bind to serum albumin with a binding constant in the range, $10^4 - 10^8 \mathrm{M}^{-1}$ (Carter and Ho, 1994) at multiple sites in a reversible manner (Curry *et al.,* 1998; Bhattacharya *et al.,* 2000; Petitpas *et al.,* 2001; Wardell *et al.,* 2002; Petitpas *et al.,* 2003; Zunszain *et al.,* 2003). Most of the ligand binding studies have been made using equilibrium dialysis or various spectroscopic methods and the binding data are generally analyzed by Scatchard method (Scatchard, 1949).

The ligand binding sites on serum albumin have been classified into two categories, site I and site II, which are located in subdomains IIA and IIIA respectively (Sudlow *et al.,* 1975). According to the Sudlow's nomenclature, site I has been characterized as a binding site for large ligands with a negative charge such as dicarboxylic acids and/or bulky heterocyclic molecules, whereas site II has been identified by the binding of aromatic carboxylic acids like non-steroidal anti-inflammatory drugs. Site I in comparison to the site II is smaller or narrower due to the binding of small ligands and seems to be less flexible (Kragh-Hansen, 1983; 1985; 1988; Yamasaki *et al.,* 1996).

Crystal structure of the subdomains containing the binding sites has shown the presence of hydrophobic side chains at the inside wall of pocket IIA whereas six positively charged residues (Arg 257, Arg 222, Lys 199, His 242, Arg 218 and Lys 195) are located at the entrance of the pocket. Similarly, IIIA pocket is also

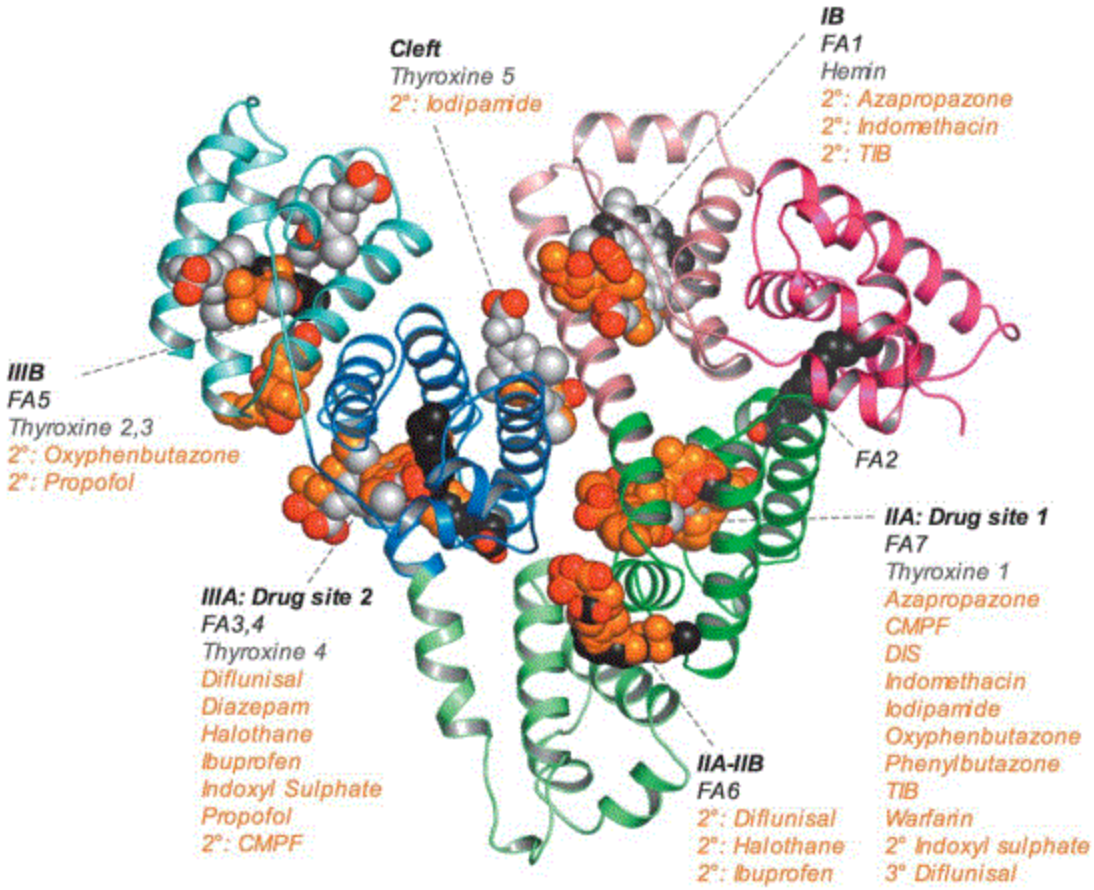

Figure 2.4 Summary of the ligand binding capacity of HSA as defined by crystallographic studies. Ligands are depicted in space filling representation; oxygen atoms are coloured red; all other atoms in fatty acids (myristic acid), other endogenous ligands (hemin, thyroxin) and drugs are coloured dark grey, light grey and orange, respectively (Taken from Ghuman *et al.*, 2005).

lined by hydrophobic side chains and the double disulfide bridges of helix IIIA−h3. Although, in both binding pockets of IIA and IIIA, the charge distribution is mostly similar but the sites still have specialized selectivity (Carter and Ho, 1994). Furthermore, the two subdomains have an asymmetric distribution, characterized by a hydrophobic surface to one side and a basic or positively charged surface on the other side (Carter and Ho, 1994).

2.5.1 Drug binding

HSA plays a central role in both efficiency and rate of drug delivery due to its drug binding properties. Protein binding not only helps in increasing the solubility of less polar compounds but also makes their distribution easier throughout the body. Therefore, such binding studies have become an important research field in chemistry, life science and clinical medicine. Many commonly used drugs such as phenylbutazone, indomethacin, aspirin, carbenicillin, warfarin, diazepam, ibuprofen etc bind to HSA, usually at one of two primary binding sites (Hultmark *et al.,* 1975; Sudlow *et al.,* 1975; He and Carter, 1992; Kosa *et al.,* 1997; Rukhadze *et al.,* 2001; Kim and Wainer, 2008; Bojko *et al.,* 2008; Thoppil *et al.,* 2008). Competitive binding experiments have been used to investigate the binding site selectivity (He and Carter, 1992; Bhattacharya *et al.,* 2000; Mao *et al.,* 2001; Petitpas *et al.,* 2001). For example, marker ligands for sites I and II of serum albumin have commonly been employed in competition experiments in order to identify the binding locus of a variety of compounds (Sudlow *et al.,* 1975; Fehske *et al.,* 1981; Kragh-Hansen, 1988; Yamasaki *et al.,* 1996). The interaction between drug and albumin has long been of interest in pharmaceutical industry

due to its importance in pharmacokinetics and pharmacodynamics of drugs (Hodgson, 2001; Rich *et al.,* 2001; Buchholz *et al.,* 2002; Kratochwil *et al.,* 2002; Valko *et al.,* 2003).

2.5.2 Warfarin binding to HSA

Warfarin [3-(α-acetonylbenzyl)-4-hydroxycoumarin], an anticoagulant drug, has been widely used in the treatment of some illnesses such as venous thrombosis and pulmonary embolism (Bell and Simon, 1982; Peterson *et al.,* 1989; Peterson and Kwaan, 1986), as well as in the prevention of prosthetic heart valve thromboembolism (Mok *et al.,* 1985). It acts by inhibiting the production of vitamin K-dependant clotting factors including, factors II, VII, IX and X (O'Reilly, 1976). The structure of warfarin is usually drawn as an open chain structure but it is generally believed to exist as a cyclic hemiketal in solution (Giannini *et al.,* 1974) and this form is the same as that observed in warfarin crystals (Valente *et al.,* 1975). Figure 2.5 shows the structure of warfarin.

Under normal therapeutic conditions, warfarin is 99% bound to the protein (HSA) in circulation (Holford and Benet, 1998). Warfarin binding to HSA has been extensively studied and the binding site of warfarin on HSA is known as the warfarin-azapropazone binding area or site I of the HSA molecule (Birkett *et al.,* 1980; Fehske *et al.,* 1981; Fehske *et al.,* 1982). This site is composed of overlapping regions for the specific binding of warfarin and other similar drugs such as coumarinic anticoagulants (Zaton *et al.,* 1995), loop diuretics (Takamura *et al.,* 1996), azapropazone, phenylbutazone and iodipamide (Yamasaki *et al.,*

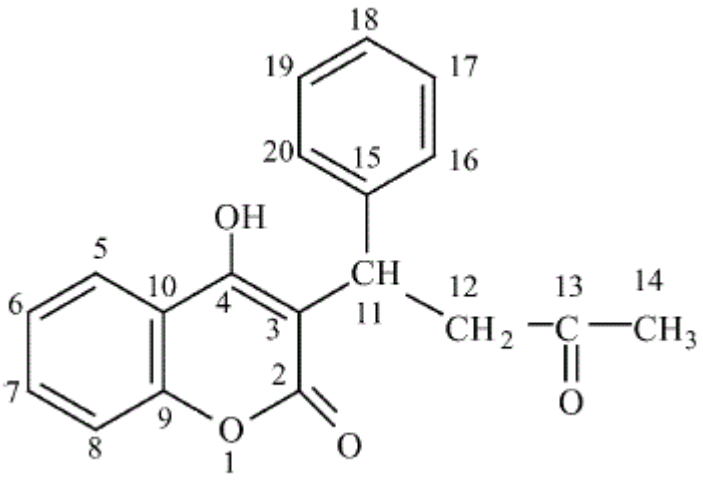

Figure 2.5 Chemical structure of warfarin [3-(α-acetonylbenzyl)-4-hydroxycoumarin].

1996). Warfarin binds to HSA with an apparent binding constant (K_b) in the range of $2.5-3.3 \times 10^5 \mathrm{M}^{-1}$ for the primary binding site (Sundlow *et al.,* 1975; Kragh-Hansen, 1981; Pinkerton and Koeplinger, 1990). Due to its specific binding to site I on HSA, warfarin is often used as a competing agent or a marker ligand for investigating the specific binding of other drugs molecules to site I on HSA (Sjoholm *et al.,* 1979; Oida, 1986; Bertucci *et al.,* 1999).

Sudlow's site I, the binding site of warfarin, has been identified as a conformationally adaptable region with up to three subcompartments and is formed as a result of packing of all six helices of subdomain IIA (Fehske *et al.,* 1981; Kragh-Hansen, 1988; He and Carter, 1992; Yamasaki *et al.,* 1996). Warfarin binding to HSA involves both hydrophobic (dominant) and electrostatic interactions. Several hydrophobic residues (Phe-211, Trp-214, Leu-219, Leu-238, Val-241, Ile-260, Ile-264, Ile-280 and Ala-291) as well as aliphatic portions of some polar residues (Arg-218, Arg-222, His-242, Arg-257 and Ser-287) in the binding pocket offer hydrophobic contacts to the incoming ligand (warfarin), whereas Arg-222 and His-242 contribute to electrostatic interactions between warfarin and HSA (Petitpas *et al.,* 2001).

It is of interest to know how warfarin or similar other drugs are transported by HSA with altered tertiary structure and to classify the drugs that protect HSA against denaturation. Furthermore, for effective therapeutic monitoring of the drug, it is necessary to know the binding parameters of drug-protein interaction during HSA destabilization as changes in the binding characteristics reflected in

the unbound drug concentration. In clinical situations, where plasma protein binding may be altered, total drug concentrations must be interpreted with caution. Although, a number of reports are available in the literature on the binding of warfarin to HSA but no attempt has been made to study the effect of chemical denaturants on the binding of warfarin to HSA. In view of the above, it would be of interest to study warfarin binding to HSA in presence of different urea concentrations. With this aim in mind, the objectives set for this study were as follows:

1. To study urea denaturation of HSA using fluorescence spectroscopy
   and
2. To compare the warfarin binding to HSA in the absence and presence of different urea concentrations.

Chapter 3

Materials and methods

MATERIALS AND METHODS

3.1 MATERIALS

Human serum albumin (HSA), essentially fatty acid free (Lot 104K7636), warfarin (minimum 98%) (Lot 104K1261), ultra pure urea (Lot 127K01061) and standard buffers of pH 7 and 4 were purchased from Sigma-Aldrich Inc., USA. Disodium hydrogen phosphate, sodium dihydrogen phosphate and sodium hydroxide were obtained from Systerm, Malaysia.

Whatman filter papers (No.1) were supplied by Whatman International Ltd., England. Parafilm 'M' was the product of American National Can Company, USA.

All glass distilled water was used throughout these studies. All experiments were performed at room temperature (~25^{o}C).

3.2. METHODS

3.2.1. pH measurements

pH measurements were made on a Mettler-Toledo pH meter, model Delta 320 using a BNC's combined electrode, type HA405-K2/120 including glass and reference electrodes in a single entity. The least count of the pH meter was 0.01 pH unit. The pH meter was calibrated at room temperature with both standard buffers of pH 7 and 4.

3.2.2. Analytical methods

Protein concentration was determined spectrophotometrically on a Shimadzu double beam Spectrophotometer, model UV-2450, using a specific extinction coefficient, $E_{279nm}^{1\%}$ of HSA as 5.31 (Janatova *et al.,* 1968).

The concentration of stock urea solution was determined from the data of Warren and Gordon (1966), as described by Pace *et al.* (1989).

3.2.3. Absorption measurements

Light absorption measurements in the ultraviolet range were carried out at 25^{O}C on a Shimadzu double beam Spectrophotometer, model UV-2450 using quartz cuvettes of 1cm path length.

3.2.4. Fluorescence measurements

Fluorescence measurements were performed on a Hitachi Fluorescence Spectrophotometer, model F-2500. Fluorescence spectra were recorded at a protein concentration of 1/ 1.8μM with a 1-cm path length cell. The excitation and emission slits were set at 10nm each. Intrinsic fluorescence was measured by exciting the protein solution at either 280 or 295nm and emission spectra were recorded in the wavelength range, 300-400nm.

3.2.5. Denaturation experiments

Urea denaturation experiments were performed in the same way as described earlier (Tayyab *et al.,* 2000). Solutions for denaturation experiments were

prepared in 0.06M sodium phosphate buffer, pH 7.4. The stock protein solution (18μM) was prepared by dissolving 29.3mg of HSA in 25ml of the same buffer. To 0.5ml of stock protein solution, different volumes of the buffer were added first followed by the addition of increasing volumes of stock denaturant solution (10M urea) to get the desired concentration of the denaturant. The final solution mixture (5ml) was incubated for 12 hours at room temperature and fluorescence spectra were recorded in the wavelength range, 300-400nm upon excitation at both 280 and 295nm. Denaturation experiments were performed at least 2-3 times and results were found reproducible.

Denaturation experiments were also performed following the above method but with 60 minutes incubation time.

3.2.6. Drug binding studies

The interaction of warfarin with HSA was studied using fluorescence spectroscopy both in the absence and presence of different urea concentrations. All experiments were carried out in 0.06M sodium phosphate buffer, pH 7.4 and at 25^{O}C.

Stock drug (400μM) and protein (18μM) solutions were prepared separately by dissolving 3.1mg of warfarin and 29.3mg of HSA in 25ml of buffer. Increasing volumes (3-500μl) of stock drug solution were added to a fixed volume (280μl/500μl) of stock protein solution, taken in different tubes and incubated for 15 minutes at room temperature. It was followed by the addition of a fixed volume of the stock denaturant solution. The final volume in each tube was made

to 5ml with buffer, if needed and the solution mixtures were incubated for additional 60 minutes at room temperature. Fluorescence spectra were recorded upon excitation at both 280 and 295nm. Same protocol was used in different experiments involving different urea concentrations.

3.2.7. Data analysis

Drug-binding data were analyzed using Stern-Volmer equation (Eftink and Ghiron, 1982).

$$F_0/F = 1 + K_{sv}\,[Q]$$

where F_0 and F are the fluorescence intensities at an appropriate wavelength in the absence and presence of drug, respectively, K_{sv} is the Stern-Volmer constant, and [Q] is the molar concentration of the drug.

Binding constant of drug-protein interaction was determined using following equation (Min *et al.,* 2004):

$$\log \frac{F_0 - F}{F} = \log K_b + \mathrm{n} \log[Q]$$

where Q is the concentration of the drug, K_b is the binding constant, n is the number of binding sites and F_0 and F are the values of fluorescence intensity in the absence and presence of drug respectively. A plot of log $[(F_0 - F)/F]$ versus log $[Q]$, gave a straight line with a slope of n and y-axis intercept of log K_b.

Chapter 4

Results and discussion

RESULTS AND DISCUSSION

4.1. EFFECT OF UREA ON THE FLUORESCENCE SPECTRUM OF HSA

4.1.1 Using excitation wavelength of 280nm

Figure 4.1 shows intrinsic fluorescence spectra of HSA (1.8μM) in the absence and presence of increasing urea concentrations (0.5-8.5M) with an incubation time of 12 hours when excited at 280nm. The fluorescence spectrum of native HSA was characterized by the presence of an emission maximum around 339nm. Addition of increasing concentrations of urea to HSA solution produced a significant decrease in the fluorescence intensity and shift in the emission maximum. Decrease in the fluorescence intensity was smaller in the beginning (0-3M), followed by a pronounced change in the middle range (3.5-6.5M) and smaller variations at higher (6.5-8.5M) urea concentrations. These changes in the fluorescence intensity can be clearly seen from Figure 4.2A where values of the fluorescence intensity at 339nm were plotted against different urea concentrations. The urea transition curve showed a two-step, three-state transition. The transition started at 3M urea and completed around 6.5M urea with the accumulation of an intermediate in the range of 5.2-5.6M urea concentrations. These results were similar to earlier reports on urea denaturation of HSA (Muzammil *et al.,* 2000; Ahmad *et al.,* 2004). In addition to the change in the fluorescence intensity, emission maximum also showed variation with increasing urea concentrations (Figure 4.2B). The emission maximum was blue shifted from

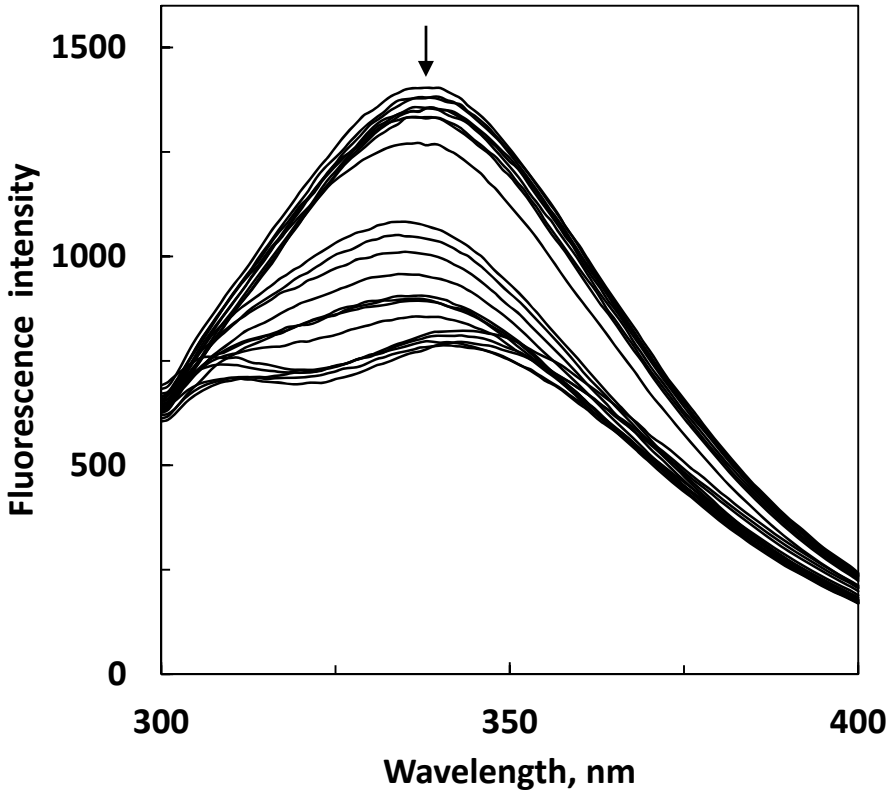

Figure 4.1 Fluorescence spectra of HSA (1.8μM) in the absence and presence of increasing urea concentrations in 0.06M sodium phosphate buffer, pH 7.0 at 25℃ incubated for 12 hours, upon excitation at 280nm. Urea concentrations from top to bottom (1-22) were: 2.0, 3.0, 1.5, 2.5, 1.0, 0.5, 0.0, 3.5, 4.0, 4.5, 4.6, 4.8, 5.0, 5.2, 5.4, 5.5, 6.0, 8.5, 6.5, 7.5, 7.0 and 8.0M respectively.

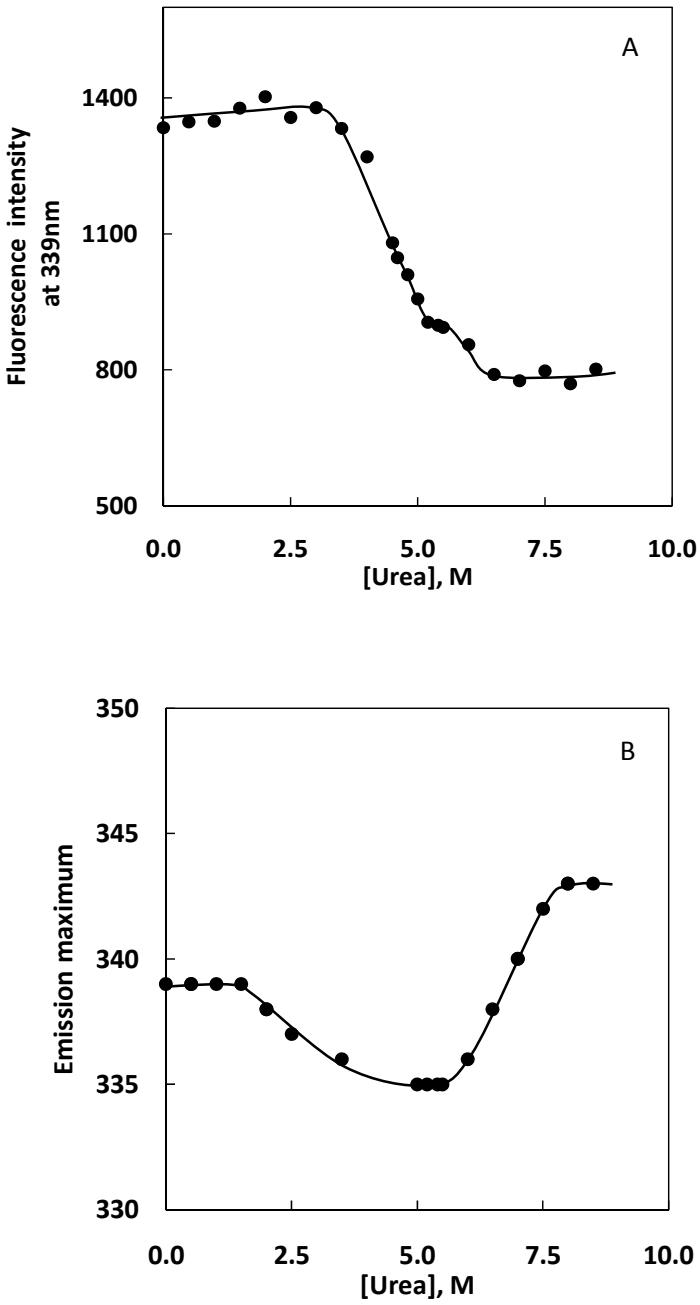

Figure 4.2 Urea denaturation curves of HSA as studied by plotting (A) fluorescence intensity at 339nm upon excitation at 280nm and (B) emission maximum against urea concentration. Data of fluorescence intensity and emission maximum at different urea concentrations were obtained from Figure 4.1.

339 to 335nm within urea concentration range, 2-5M, remained constant till 5.5M urea and then showed a red shift of 8.0nm till 8.0M and became constant thereafter.

Decrease in the fluorescence intensity observed within urea concentration range, 3.5-6.5M, can be ascribed to the change in the microenvironment around tryptophan (Trp) and tyrosine (Tyr) residues of HSA from nonpolar to polar (Rownicka *et al.,* 2006). These results were supported by the significant red shift observed with increasing urea concentrations (Figure 4.2B). Both decrease in the fluorescence intensity and red shift in the emission maximum were suggestive of protein denaturation. Furthermore, the fluorescence spectrum of HSA showed two emission maxima at 307 and 343nm at higher (>6M) urea concentrations (Figure 4.1). Presence of emission maximum at 307nm can account for Tyr fluorescence whereas emission maximum at 343nm corresponds to Trp fluorescence (Ahmad *et al.,* 2005; Rownicka *et al.,* 2006; Qu *et al.,* 2009). HSA contains 18 Tyr residues, distributed in all three domains and single Trp residue, localized in subdomain IIA (Minghetti *et al.,* 1986). Tyrosine fluorescence remains quenched in the native three-dimensional structure of the protein due to the presence of Trp residue (Rownicka-zubik *et al.,* 2009). Denaturation at higher urea concentrations led to the separation of Tyr and Trp residues, thus leading to the appearance of two maxima in the fluorescence spectrum of HSA. Origin of a new peak at 307nm can also account for the smaller decrease in emission maximum observed at lower urea concentrations (Figure 4.2B).

In order to study the effect of 60 minutes incubation time on the urea denaturation characteristics of HSA, denaturation experiments were also performed using 60 minutes incubation time with urea. Figure 4.3A and B show urea denaturation curves of HSA when monitored by fluorescence intensity at emission maximum (338nm) and emission maximum respectively. As can be seen from the figure, transition curves were found to be similar to those obtained with 12 hours incubation (Figure 4.2A and B).

4.1.2 Using excitation wavelength of 295nm

Urea denaturation studies of HSA were also made using fluorescence spectroscopy upon excitation at 295nm (to excite Trp residues only) with an incubation time of 12 hours. Figure 4.4 shows fluorescence spectra of HSA (1.8μM) both in the absence and presence of increasing (0-8M) urea concentrations when excited at 295nm. Fluorescence spectrum of HSA showed an emission maximum at 343nm. Addition of increasing urea concentrations resulted in quenching of Trp fluorescence as well as red shift in the emission maximum. These changes were more visible in Figure 4.5A and B where fluorescence intensity at 338nm and emission maximum respectively have been plotted against urea concentrations. However, these effects were smaller both at lower (0-3M) and higher (6-8M) urea concentrations and became more pronounced in the middle range, 3-6M, of urea concentrations (Figure 4.5A). Urea denaturation of HSA showed a single-step, two-state transition when monitored by Trp fluorescence. The transition was characterized by the start- and end-points at 3M and 6M urea respectively. Similarly, urea denaturation curve probed by emission

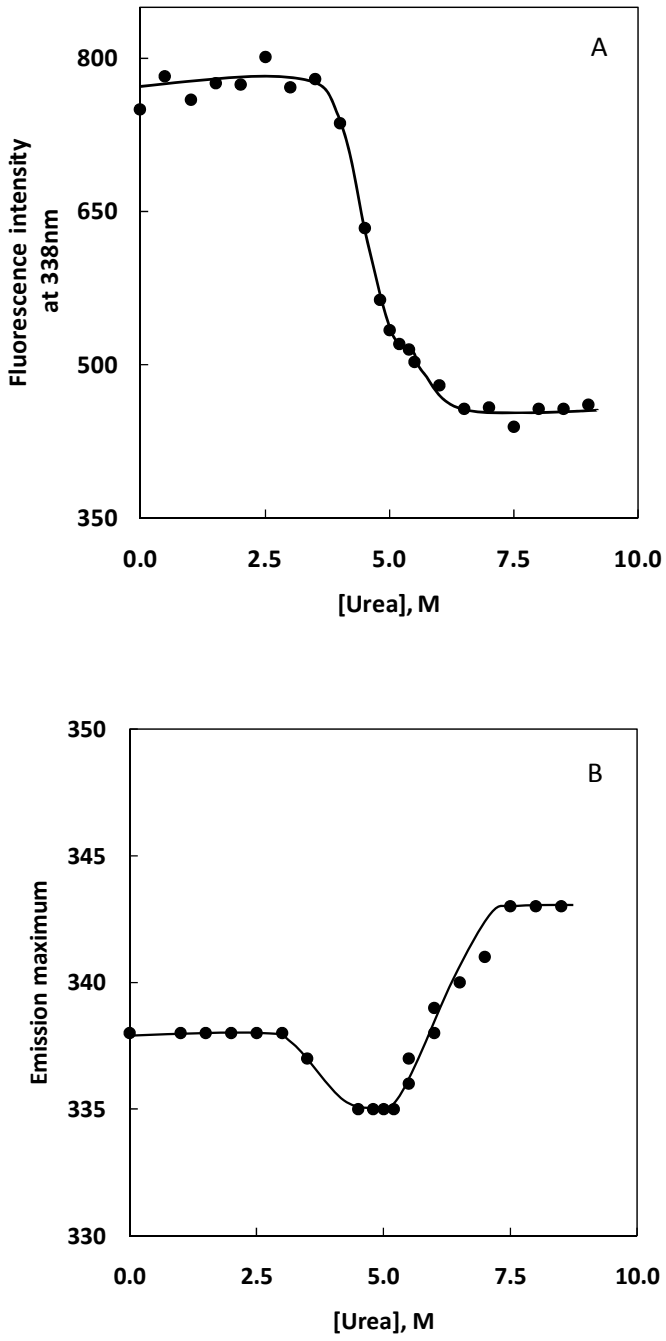

Figure 4.3 Urea denaturation curves of HSA (1.0μM) as studied by plotting (A) fluorescence intensity at 338nm upon excitation at 280nm and (B) emission maximum against urea concentration. Incubation time with urea was kept as 60 minutes.

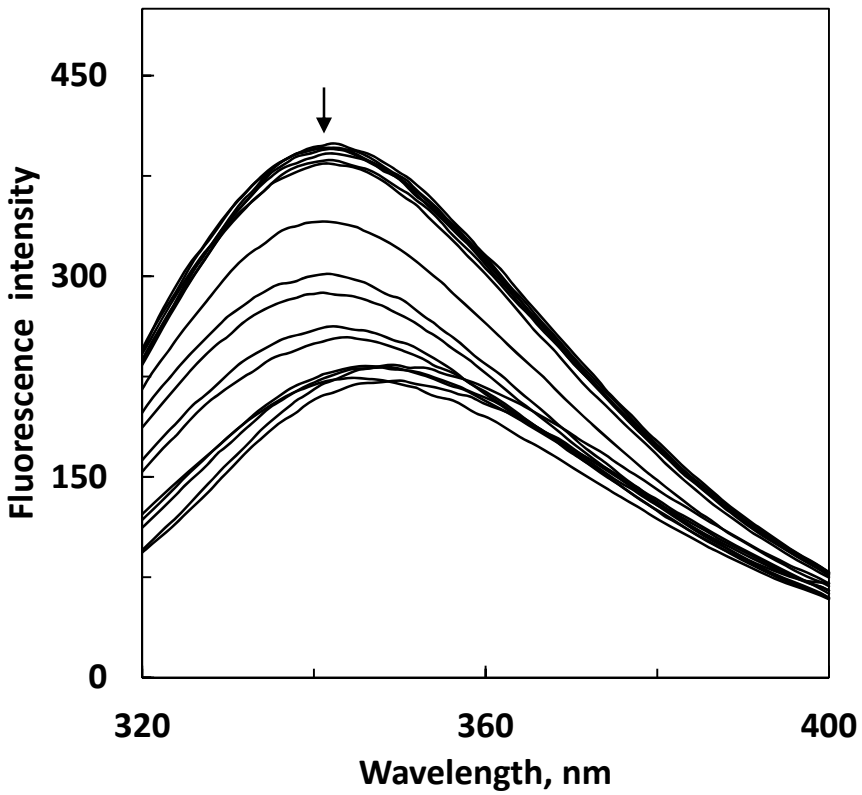

Figure 4.4 Fluorescence spectra of HSA (1.8μM) in the absence and presence of increasing urea concentrations in 0.06M sodium phosphate buffer, pH 7.0 at 25℃ incubated for 12 hours, upon excitation at 295nm. Urea concentrations from top to bottom (1-17) were: 1.5, 0.5, 3.0, 2.0, 1.0, 3.5, 0.0, 4.0, 4.6, 4.8, 5.2, 5.5, 6.5, 7.0, 6.0, 8.0 and 7.5M respectively.

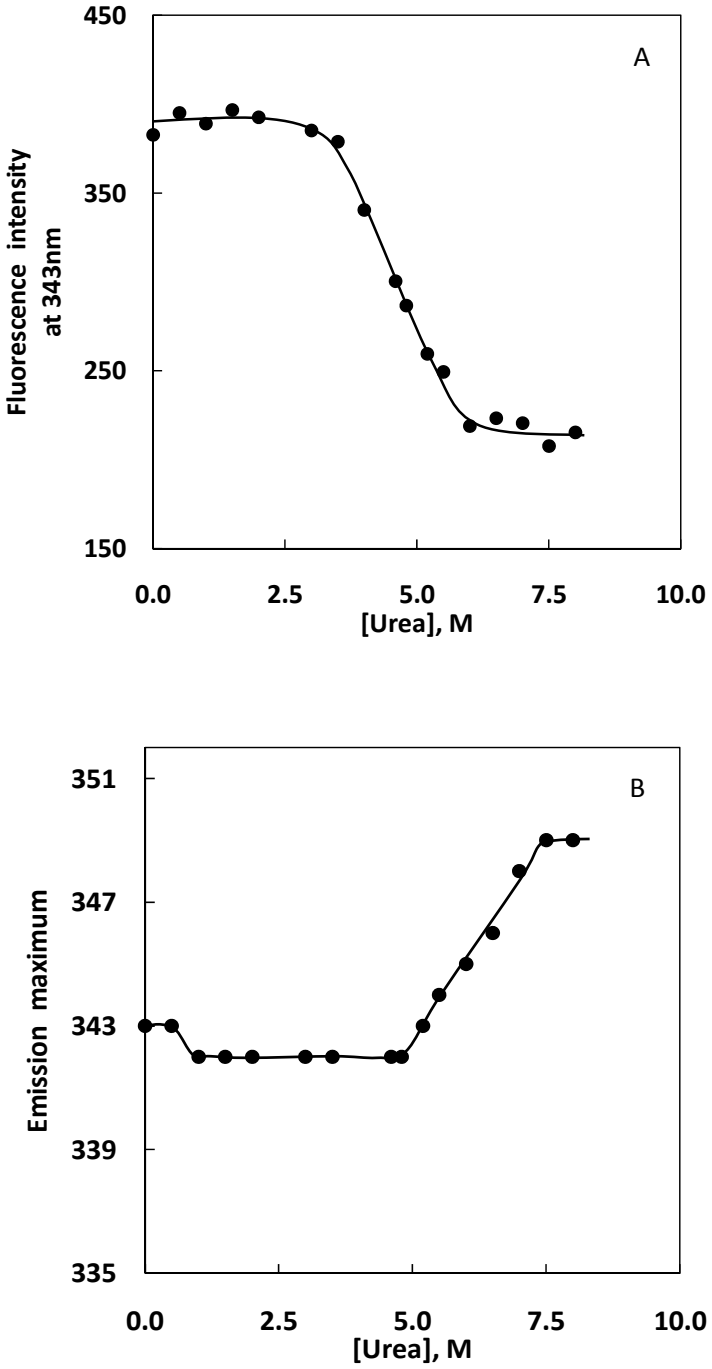

Figure 4.5 Urea denaturation curves of HSA as studied by plotting (A) fluorescence intensity at 343nm upon excitation at 295nm and (B) emission maximum against urea concentration. Data of fluorescence intensity and emission maximum at different urea concentrations were obtained from Figure 4.4.

maximum also showed a single-step transition starting at 5M urea and reaching to completion at 7.5M urea (Figure 4.5B). Use of different probes may account for the observed differences in the start- and end-points of transitions. Since HSA contains single Trp residue, located at 214 position in the primary sequence (domain II), urea denaturation of HSA monitored by Trp fluorescence would account for the denaturation of the concerned domain only and thus resulted in a single-step transition as shown in Figure 4.5. Contrary to it, excitation at 280nm was responsible to excite both Tyr and Trp residues of HSA. Since Tyr residues are scattered throughout the three domains of HSA molecule, probing urea denaturation of HSA with intrinsic fluorescence would give denaturation details of all three domains of HSA. That is why the urea denaturation of HSA showed two-step transition when probed by intrinsic fluorescence. Decreasing the incubation time from 12 hours to 60 minutes did not affect the transition curves to a significant extent (Figure 4.6).

4.2. WARFARIN-HSA INTERACTION

4.2.1 Warfarin binding to native HSA

Intrinsic fluorescence spectra of HSA (1μM) both in the absence and presence of increasing warfarin concentrations (1-40μM) upon excitation at 280nm are shown in Figure 4.7. As can be seen from the figure, native HSA produced the fluorescence spectrum in the wavelength range, 300-400nm with an emission maximum at 338nm. Appearance of an emission maximum at 338nm was indicative of the presence of Trp residue in HSA (Muzammil *et al.,* 2000; Ahmad

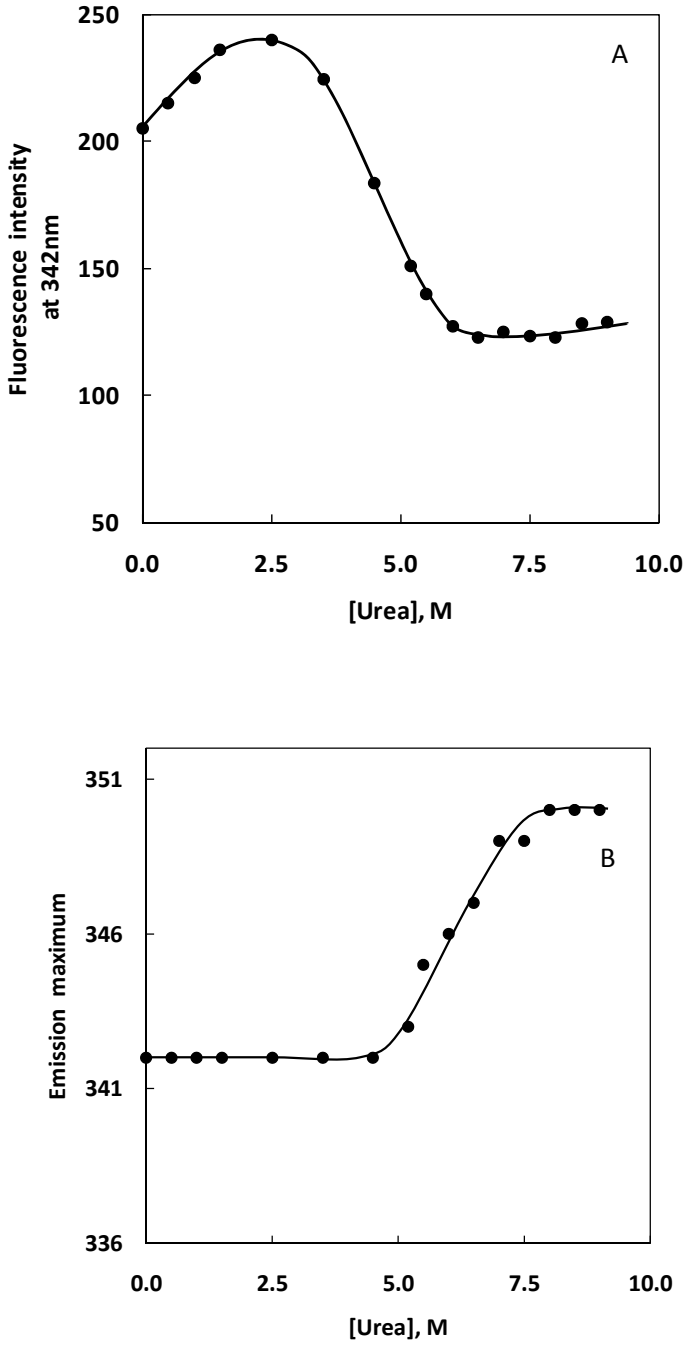

Figure 4.6 Urea denaturation curves of HSA (1.0μM) as studied by plotting (A) fluorescence intensity at 342nm upon excitation at 295nm and (B) emission maximum against urea concentration. Incubation time with urea was kept as 60 minutes.

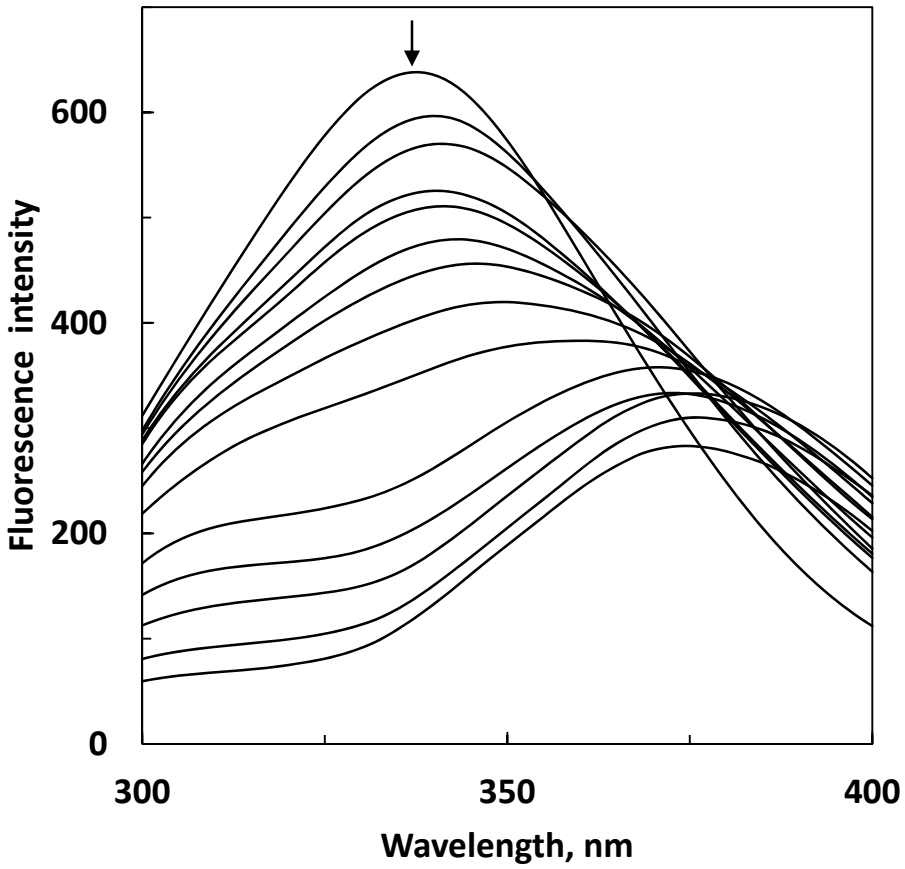

Figure 4.7 Fluorescence spectra of HSA (1.0μM) in the absence and presence of increasing warfarin concentrations in 0.06M sodium phosphate buffer, pH 7.0 at 25℃ incubated for 60 minutes, upon excitation at 280nm. Warfarin concentrations from top to bottom (1-14) were: 0.0, 1.0, 1.3, 1.6, 2.0, 2.5, 3.0, 4.0, 5.0, 10.0, 15.0, 20.0, 30.0 and 40.0μM respectively.

et al., 2005). Both decrease in the fluorescence intensity and red shift in the emission maximum were observed in the fluorescence spectrum of HSA in presence of increasing warfarin concentrations (Figure 4.7). These effects were more pronounced at lower (0-5μM) drug concentrations and sloped off at higher (10-40μM) drug concentrations. This can be clearly seen from Figure 4.8A and B where relative fluorescence intensity at 338nm (obtained by taking the fluorescence intensity of native HSA at 338nm, in the absence of drug as 100) and emission maximum respectively were plotted against drug concentration. About 45% quenching in the fluorescence intensity was observed up to a warfarin/ HSA molar ratio of 5:1. Further increase in the drug concentration from 5 to 40μM led to only 35% quenching in the fluorescence intensity, being 80% at 40μM drug concentration (Figure 4.8A).

Similarly, red shift in the emission maximum was more marked (22nm) at 5μM drug concentration and became smaller at higher drug concentrations. The value of emission maximum reached to 376nm at 20μM drug concentration and remained the same (within experimental error) up to 40μM drug concentration (Figure 4.8B). Both decrease in the fluorescence intensity and red shift in the emission maximum of HSA with increasing warfarin concentrations were indicative of warfarin binding to HSA. Binding of warfarin to HSA has been well studied using different techniques including fluorescence spectroscopy and our results were found to be in agreement to those published earlier (Parikh *et al.,* 2000; Sulkowska, 2002; Sulkowska *et al.,* 2003). Linear decrease in the fluorescence intensity at lower drug concentrations and saturation at higher drug concentrations

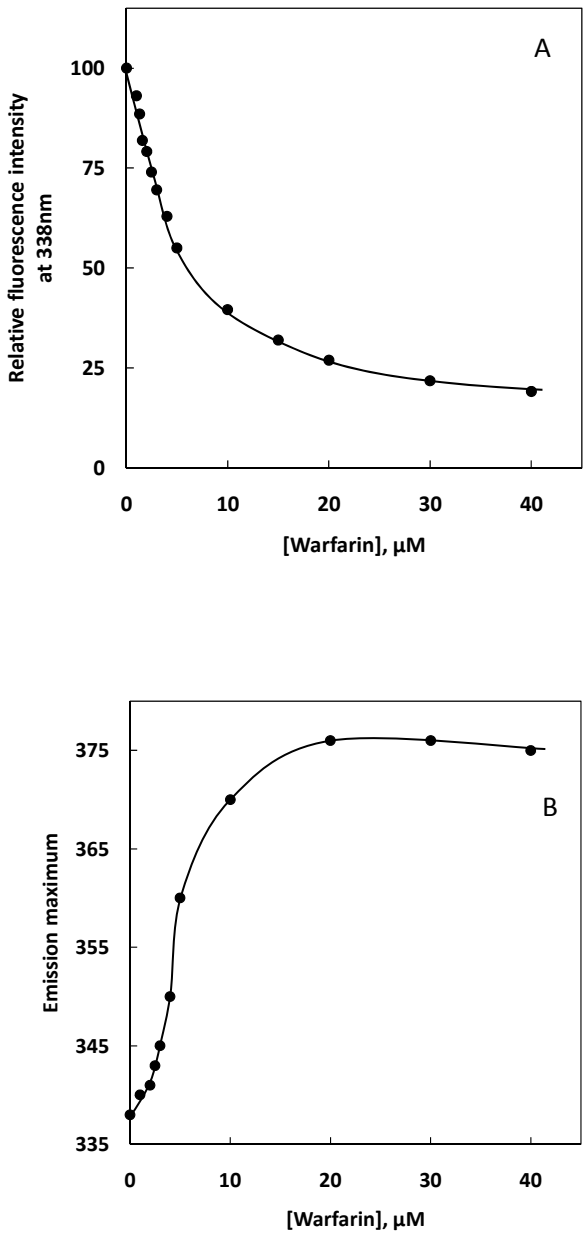

Figure 4.8 Plots showing change in the relative fluorescence intensity at 338nm upon excitation at 280nm (A) and the emission maximum (B) of HSA against warfarin concentration. Data of the relative fluorescence intensity and the emission maximum at different warfarin concentrations were obtained from Figure 4.7.

are typical for specific ligand binding to proteins (Tayyab *et al.,* 2000; Ahmad *et al.,* 2004).

Warfarin binding to HSA was also studied using Trp fluorescence upon excitation at 295nm and results are shown in Figure 4.9. The fluorescence spectrum of native HSA was characterized by the presence of an emission maximum at 342nm which was in line with previous reports (Muzammil *et al.,* 2000; Ahmad *et al.,* 2004). A comparison of the emission maximum of free Trp in buffer (354nm) (Pajot, 1976), with that (342nm) obtained with HSA suggested the internalization of Trp in the hydrophobic interior of the protein (Pajot, 1976; Moller and Denicola, 2002). Addition of increasing warfarin concentrations to the HSA solution led to a significant decrease in the fluorescence intensity and red shift in the emission maximum. These results on the change in the fluorescence intensity and emission maximum with increasing warfarin concentrations (Figure 4.10A and B) were found to be similar to those observed upon excitation at 280nm (Figure 4.8A and B). The extent of fluorescence quenching and red shift at 5μM drug concentration were found as 49% and 31nm respectively and followed the linear pattern in the beginning (Figure 4.10A and B). Similarly, at 40μM drug concentration, about 79% quenching of Trp fluorescence and 39nm red shift in the emission maximum (Figure 4.10A and B) were observed against 80% quenching and 37nm red shift (Figure 4.8A and B) noted upon excitation at 280nm.

In view of the similar extent of fluorescence quenching observed in the presence of warfarin, upon excitation at 280 and 295nm (Figure 4.8A and 10A), it seems

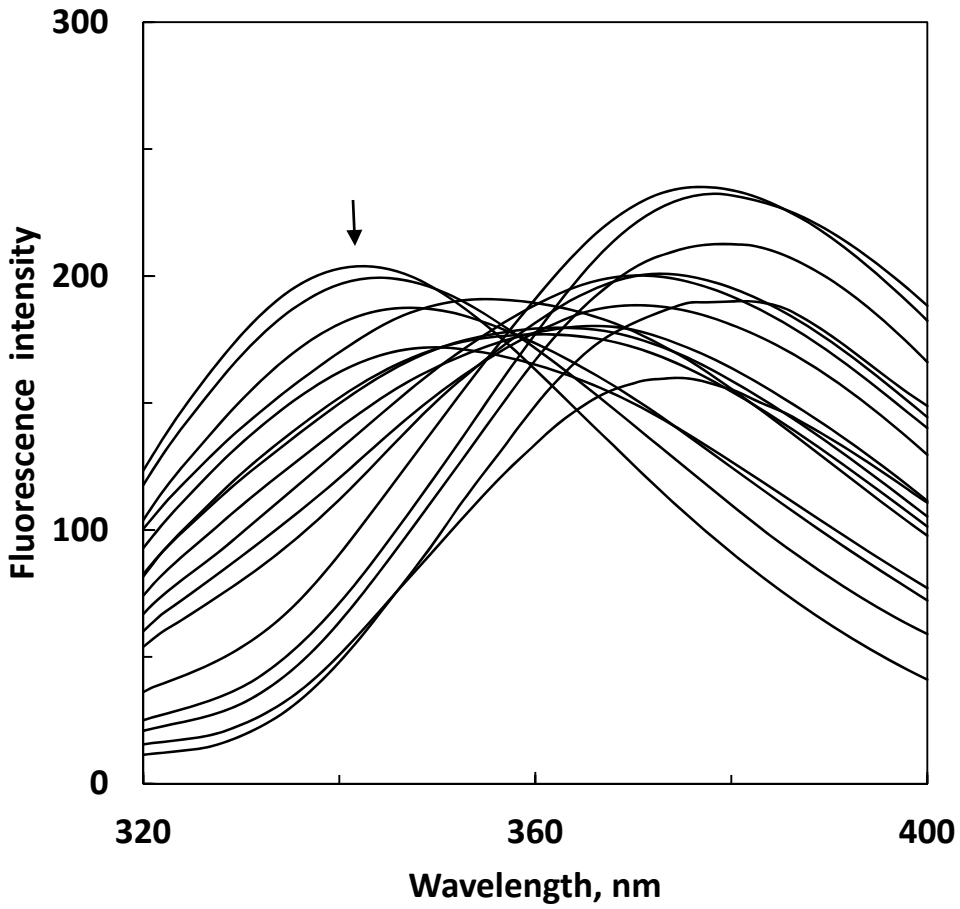

Figure 4.9 Fluorescence spectra of HSA (1.0μM) in the absence and presence of increasing warfarin concentrations in 0.06M sodium phosphate buffer, pH 7.0 at 25℃ incubated for 60 minutes, upon excitation at 295nm. Warfarin concentrations from top to bottom (1-16) were: 0.0, 0.24, 0.75, 1.0, 1.3, 1.6, 2.0, 2.5, 3.0, 3.5, 5.0, 10.0, 15.0, 20.0, 30.0 and 40.0μM respectively.

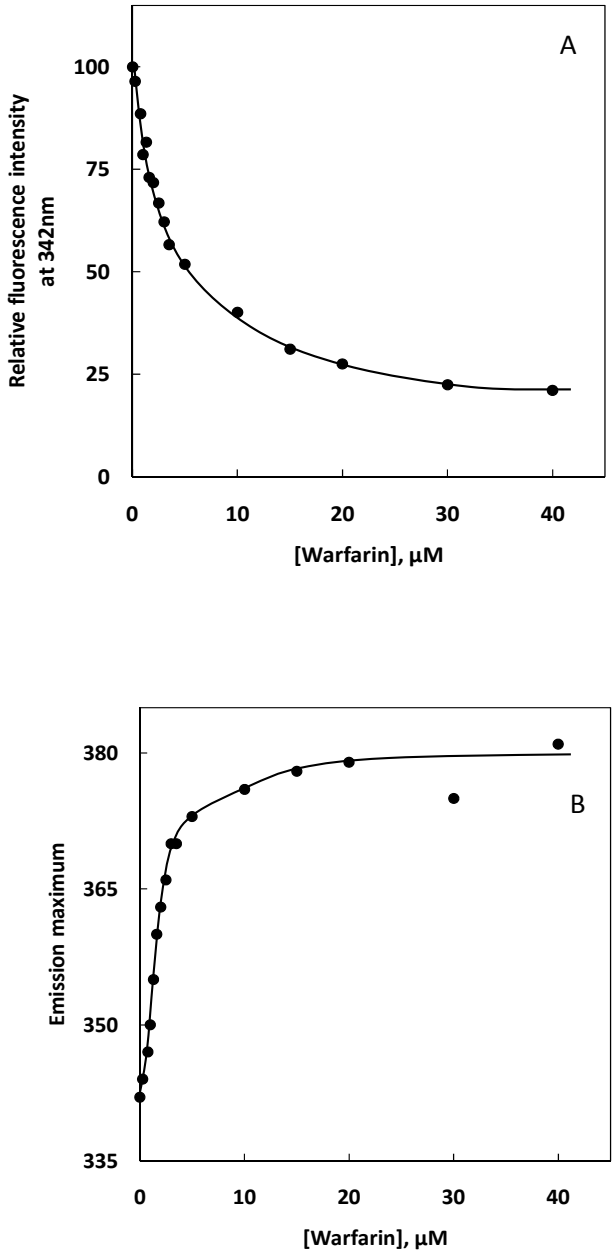

Figure 4.10 Plots showing change in the relative fluorescence intensity at 342nm upon excitation at 295nm (A) and the emission maximum (B) of HSA against warfarin concentration. Data of the relative fluorescence intensity and the emission maximum at different warfarin concentrations were obtained from Figure 4.9.

likely that both fluorophores, Trp and Tyr are involved in the drug binding to HSA. The quenching of HSA fluorescence can be explained by the energy transfer from the fluorophores to the drug molecule in its ground state. Free warfarin absorbs in the ultraviolet range with an absorption maximum around 306nm (Corn and Berberich, 1967). The possibility of energy transfer is more if the emission spectrum of HSA (donor) overlaps the absorption spectrum of the drug (acceptor) (Valeur, 2002). This condition is met in warfarin-HSA system as there is significant overlap between absorption spectrum of warfarin and emission spectrum of HSA (Figure omitted for brevity). Furthermore, increase in the polarity of the microenvironment around Trp and Tyr residues was also reflected by the decrease in the fluorescence intensity and red shift in the emission maximum of HSA in the presence of warfarin. The fluorescence quenching of Trp residue upon excitation at 295nm suggested the location of warfarin binding site close to Trp-214 in subdomain IIA of HSA (Tanaka *et al.,* 1997; Rownicka-Zubik *et al.,* 2009). Since drug site I, available in subdomain IIA of HSA contains a hydrophobic pocket surrounded by polar clusters (Ghuman *et al.,* 2005), warfarin binding to this site might have brought a conformational change leading to increased polarity around Trp-214. In class B proteins, Trp residue(s) is(are) solely responsible for fluorescence even in the presence of a higher number of Tyr residues due to quenching of Tyr fluorescence by Trp and/or energy transfer from Tyr to Trp in the native structure of a protein where these residues are closely located (Weber, 1960).

4.2.2 Warfarin binding to HSA in the presence of urea

Interaction of warfarin with HSA was also studied in the presence of different urea concentrations *i.e.*: 3.0, 3.5, 4.0, 4.5, 5.3, 6.5 and 8.0M using fluorescence spectroscopy. Titration of a constant amount of HSA (1/1.8μM) was performed with increasing warfarin concentrations (0.5-40μM) in the presence of fixed urea concentration and the resulting fluorescence spectra are shown in Figures 4.11, 4.13, 4.15, 4.17, 4.19, 4.21 and 4.23 upon excitation at 280nm. Fluorescence spectra obtained in the presence of different urea concentrations were found to be qualitatively similar to that observed in the absence of urea (Figure 4.7) in terms of both decrease in the fluorescence intensity and red shift in the emission maximum. However, significant differences in the extent of fluorescence quenching as well as red shift in the emission maximum were noticed with different urea concentrations. This can be more clearly seen from the plots of relative fluorescence intensity and emission maximum against warfarin concentration as shown in Figures 4.12, 4.14, 4.16, 4.18, 4.20, 4.22 and 4.24. A comparison of these plots obtained at different urea concentrations showed a significant decrease both in the extent of fluorescence quenching (Figure 4.25A) and red shift in the emission maximum (Figure 4.26A) with the increase in urea concentration.

The pattern of fluorescence quenching with increasing warfarin concentrations remained the same at lower urea concentrations, showing marked decrease in the fluorescence intensity at lower drug concentrations and smaller decrease at higher

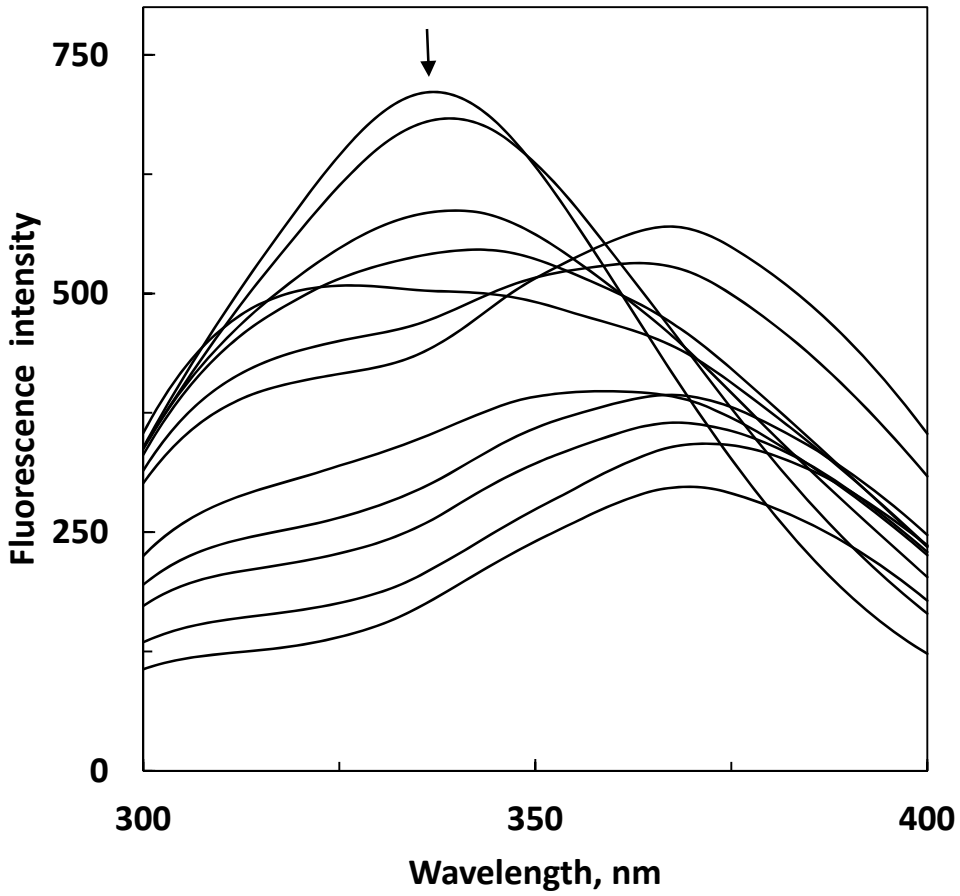

Figure 4.11 Fluorescence spectra of HSA (1.0μM) in the absence and presence of increasing warfarin concentrations but with 3.0M urea in 0.06M sodium phosphate buffer, pH 7.0 at 25℃ incubated for 60 minutes, upon excitation at 280nm. Warfarin concentrations from top to bottom (1-12) were: 0.0, 0.75, 1.0, 1.3, 1.6, 2.5, 3.5, 10.0, 15.0, 20.0, 30.0 and 40.0μM respectively.

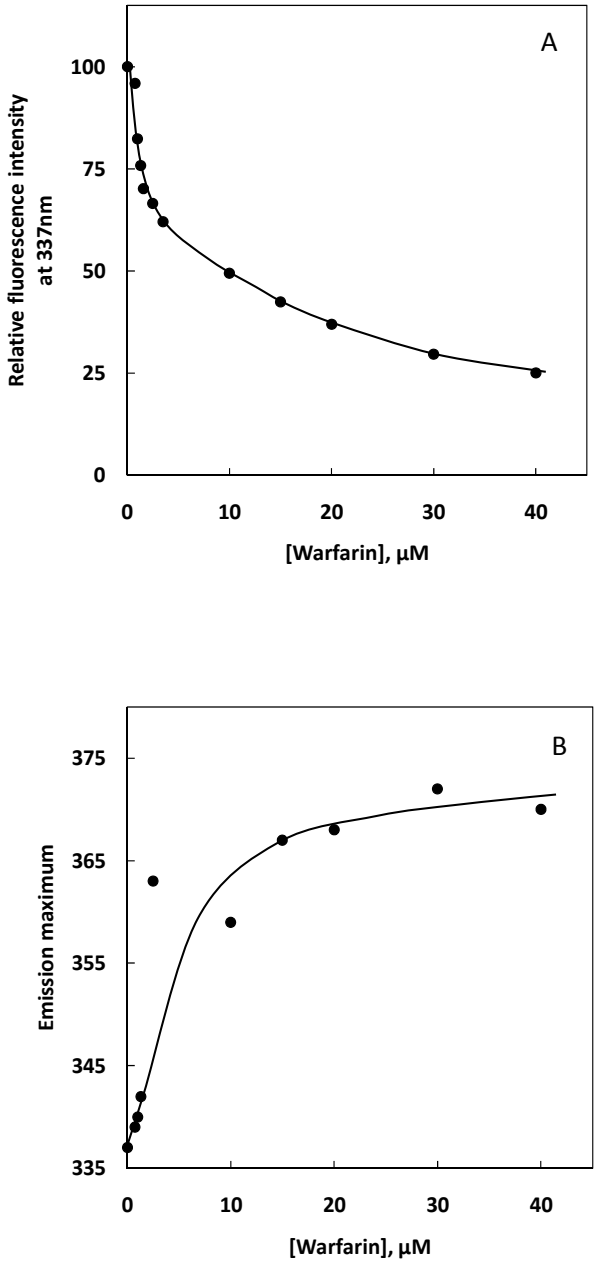

Figure 4.12 Plots showing change in the relative fluorescence intensity at 337nm upon excitation at 280nm (A) and the emission maximum (B) of HSA in 3.0M urea against warfarin concentration. Data of the relative fluorescence intensity and the emission maximum at different warfarin concentrations were obtained from Figure 4.11.

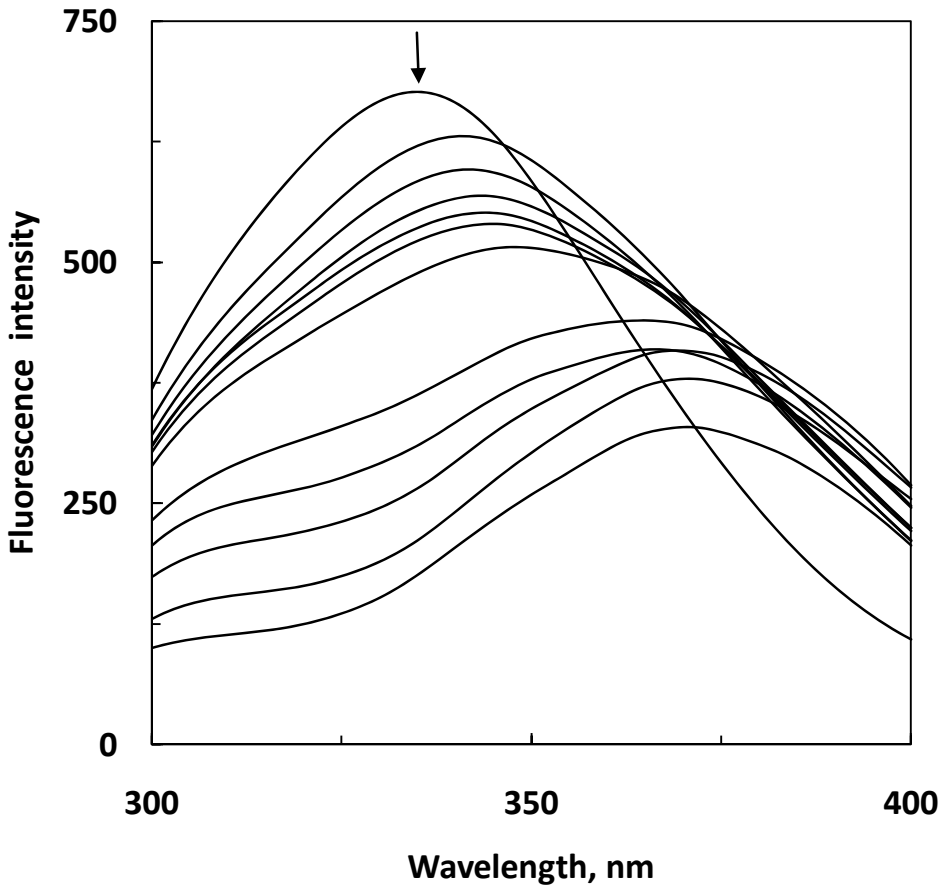

Figure 4.13 Fluorescence spectra of HSA (1.0μM) in the absence and presence of increasing warfarin concentrations but with 3.5M urea in 0.06M sodium phosphate buffer, pH 7.0 at 25℃ incubated for 60 minutes, upon excitation at 280nm. Warfarin concentrations from top to bottom (1-14) were: 0.0, 2.0, 2.5, 3.0, 3.5, 4.0, 5.0, 10.0, 15.0, 20.0, 30.0 and 40.0μM respectively.

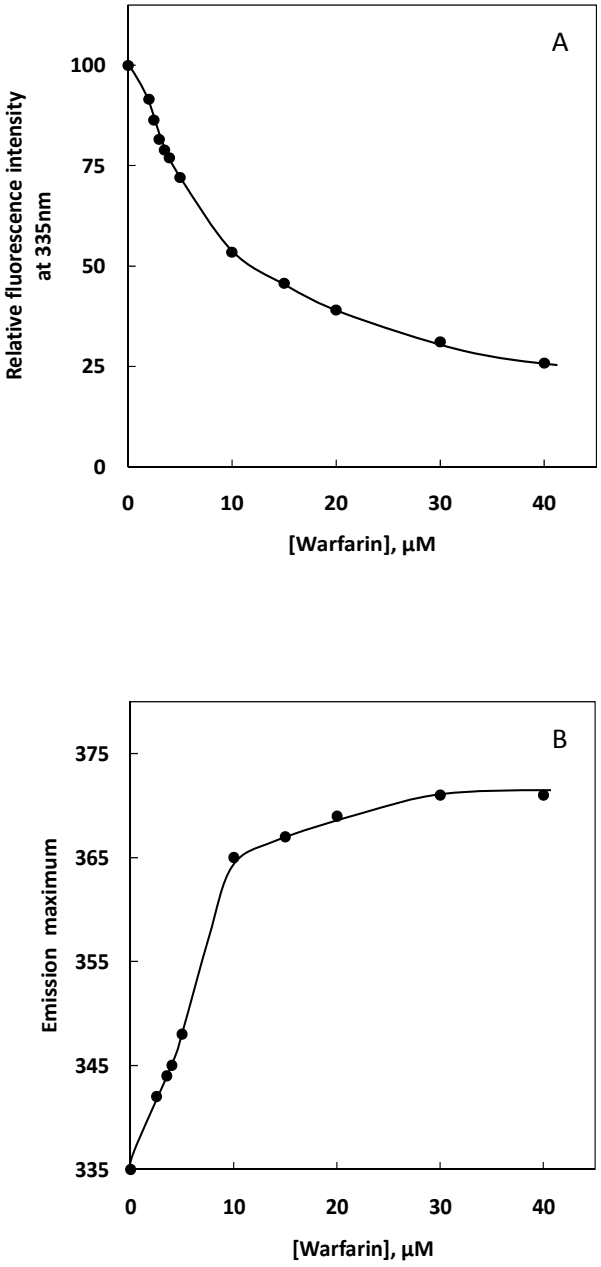

Figure 4.14 Plots showing change in the relative fluorescence intensity at 335nm upon excitation at 280nm (A) and the emission maximum (B) of HSA in 3.5M urea against warfarin concentration. Data of the relative fluorescence intensity and the emission maximum at different warfarin concentrations were obtained from Figure 4.13.

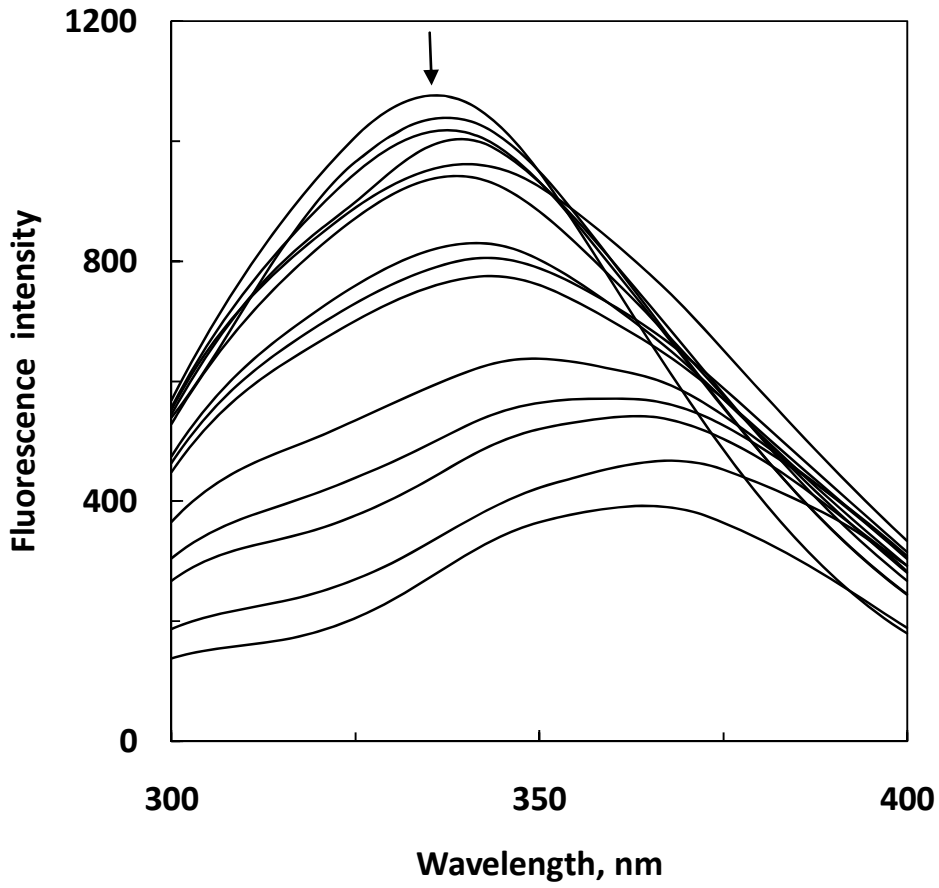

Figure 4.15 Fluorescence spectra of HSA (1.8μM) in the absence and presence of increasing warfarin concentrations but with 4.0M urea in 0.06M sodium phosphate buffer, pH 7.0 at 25℃ incubated for 60 minutes, upon excitation at 280nm. Warfarin concentrations from top to bottom (1-15) were: 0.0, 0.75, 1.0, 1.3, 1.6, 2.0, 3.5, 4.0, 5.0, 10.0, 15.0, 20.0, 30.0 and 40.0μM respectively.

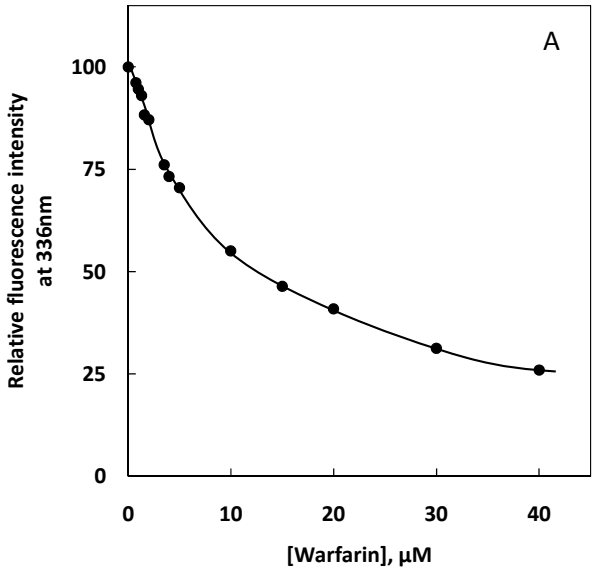

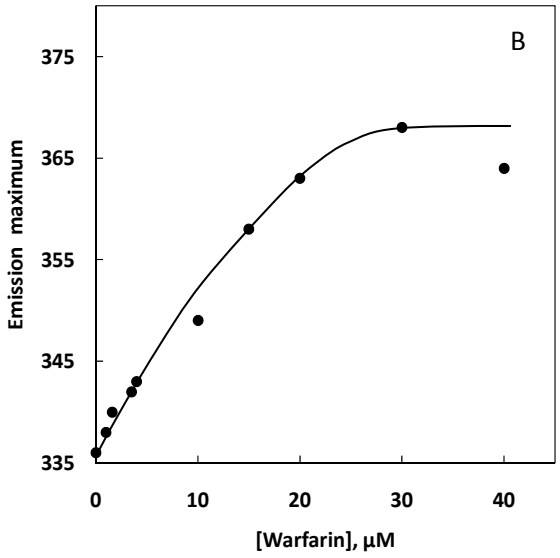

Figure 4.16 Plots showing change in the relative fluorescence intensity at 336nm upon excitation at 280nm (A) and the emission maximum (B) of HSA in 4.0M urea against warfarin concentration. Data of the relative fluorescence intensity and the emission maximum at different warfarin concentrations were obtained from Figure 4.15.

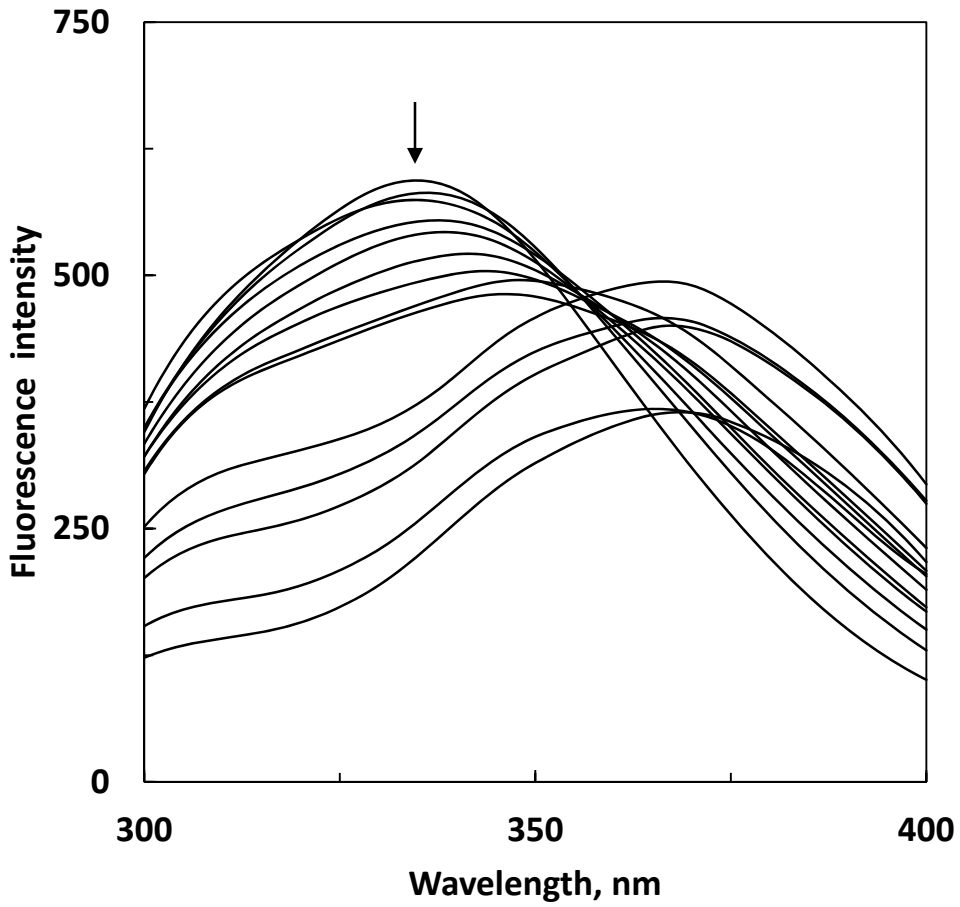

Figure 4.17 Fluorescence spectra of HSA (1.0μM) in the absence and presence of increasing warfarin concentrations but with 4.5M urea in 0.06M sodium phosphate buffer, pH 7.0 at 25℃ incubated for 60 minutes, upon excitation at 280nm. Warfarin concentrations from top to bottom (1-14) were: 0.0, 0.5, 0.75, 1.0, 1.3, 1.6, 2.0, 3.0, 3.5, 10.0, 15.0, 20.0, 30.0 and 40.0μM respectively.

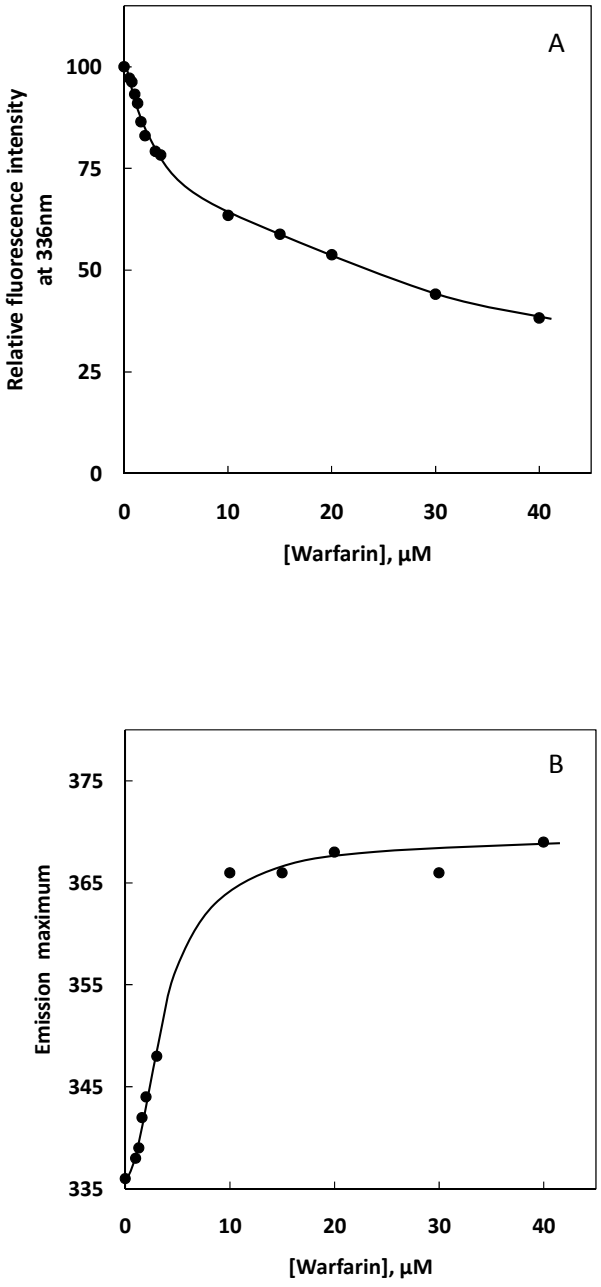

Figure 4.18 Plots showing change in the relative fluorescence intensity at 336nm upon excitation at 280nm (A) and the emission maximum (B) of HSA in 4.5M urea against warfarin concentration. Data of the relative fluorescence intensity and the emission maximum at different warfarin concentrations were obtained from Figure 4.17.

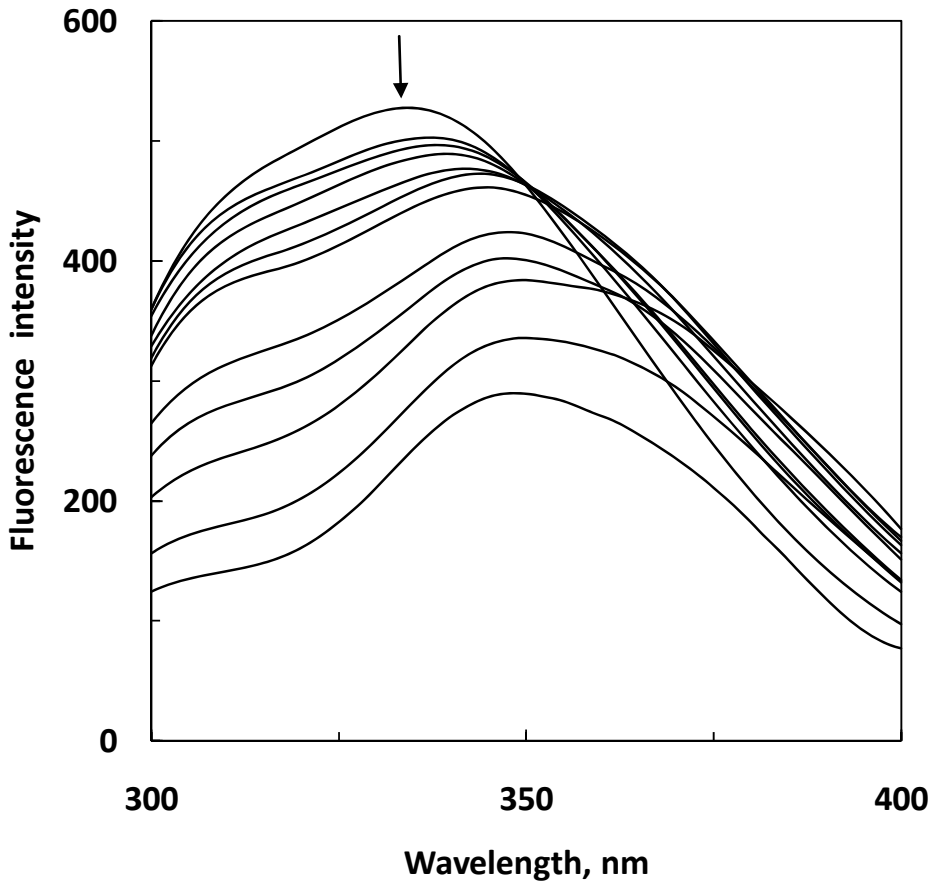

Figure 4.19 Fluorescence spectra of HSA (1.0μM) in the absence and presence of increasing warfarin concentrations but with 5.3M urea in 0.06M sodium phosphate buffer, pH 7.0 at 25℃ incubated for 60 minutes, upon excitation at 280nm. Warfarin concentrations from top to bottom (1-13) were: 0.0, 1.0, 1.3, 1.6, 3.0, 4.0, 5.0, 10.0, 15.0, 20.0, 30.0 and 40.0μM respectively.

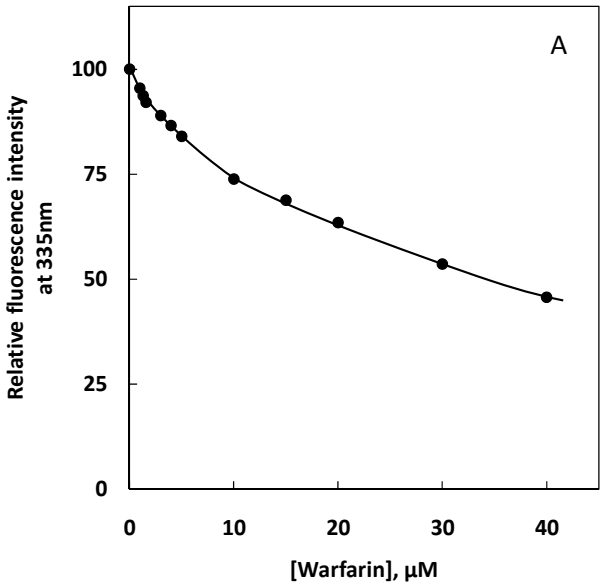

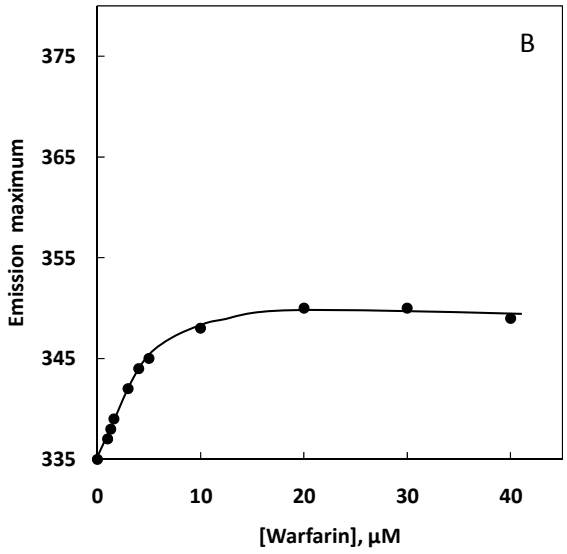

Figure 4.20 Plots showing change in the relative fluorescence intensity at 335nm upon excitation at 280nm (A) and the emission maximum (B) of HSA in 5.3M urea against warfarin concentration. Data of the relative fluorescence intensity and the emission maximum at different warfarin concentrations were obtained from Figure 4.19.

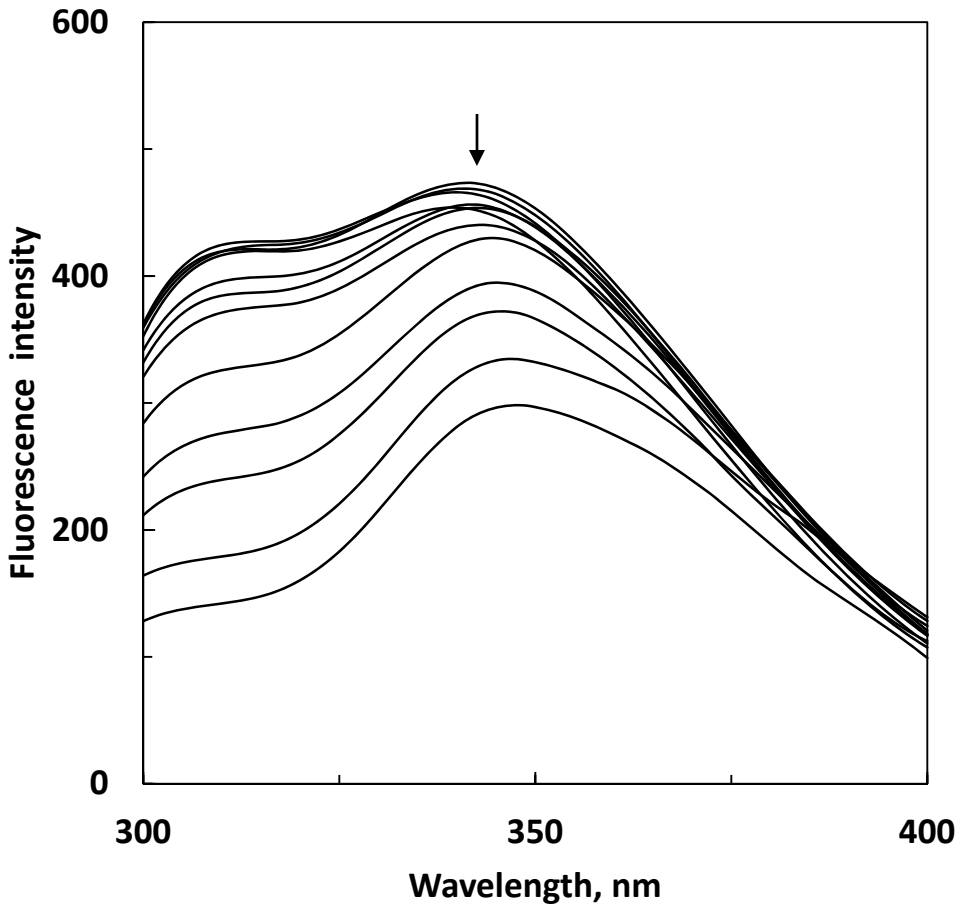

Figure 4.21 Fluorescence spectra of HSA (1.0μM) in the absence and presence of increasing warfarin concentrations but with 6.5M urea in 0.06M sodium phosphate buffer, pH 7.0 at 25℃ incubated for 60 minutes, upon excitation at 280nm. Warfarin concentrations from top to bottom (1-12) were: 0.0, 0.5, 1.6, 2.5, 3.5, 4.0, 5.0, 10.0, 15.0, 20.0, 30.0 and 40.0μM respectively.

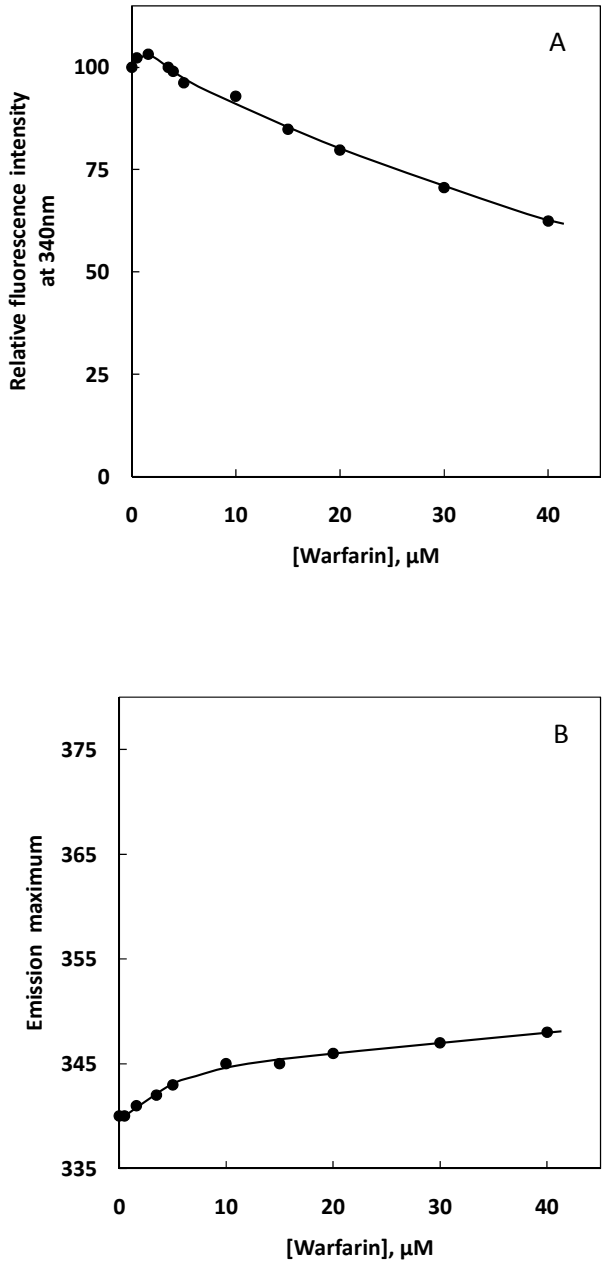

Figure 4.22 Plots showing change in the relative fluorescence intensity at 340nm upon excitation at 280nm (A) and the emission maximum (B) of HSA in 6.5M urea against warfarin concentration. Data of the relative fluorescence intensity and the emission maximum at different warfarin concentrations were obtained from Figure 4.21.

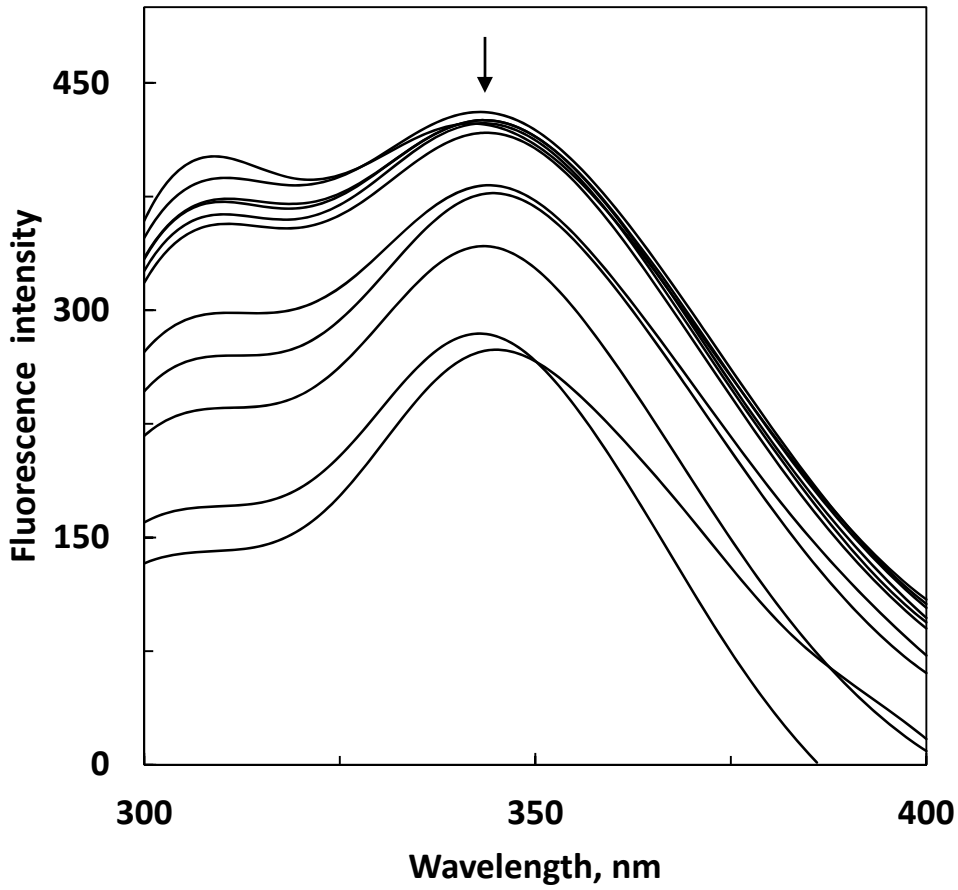

Figure 4.23 Fluorescence spectra of HSA (1.0μM) in the absence and presence of increasing warfarin concentrations but with 8.0M urea in 0.06M sodium phosphate buffer, pH 7.0 at 25℃ incubated for 60 minutes, upon excitation at 280nm. Warfarin concentrations from top to bottom (1-11) were: 0.0, 0.75, 3.0, 3.5, 4.0, 5.0, 10.0, 15.0, 20.0, 30.0 and 40.0μM respectively.

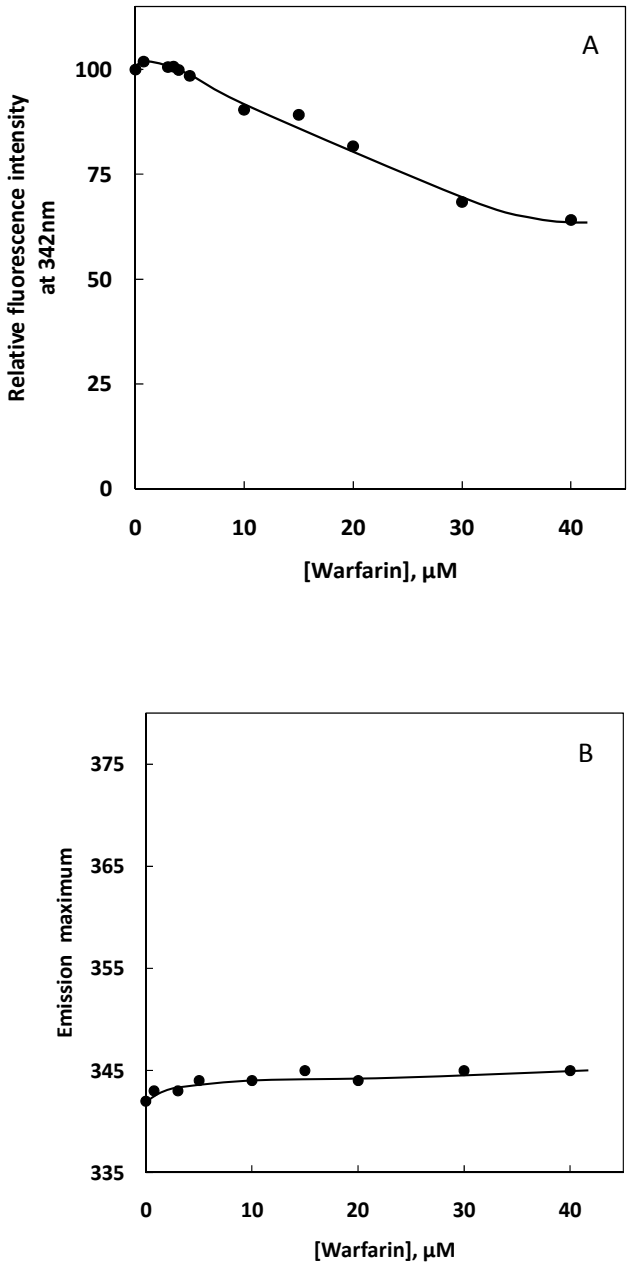

Figure 4.24 Plots showing change in the relative fluorescence intensity at 342nm upon excitation at 280nm (A) and the emission maximum (B) of HSA in 8.0M urea against warfarin concentration. Data of the relative fluorescence intensity and emission maximum at different warfarin concentrations were obtained from Figure 4.23.

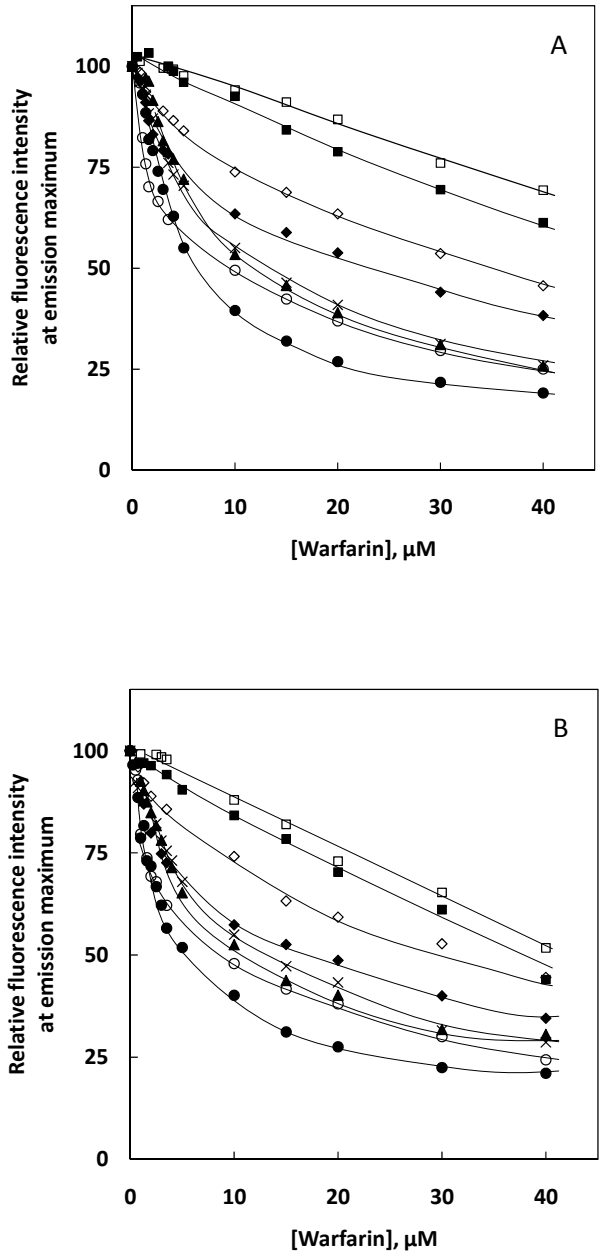

Figure 4.25 Plots showing change in the relative fluorescence intensity of HSA at the emission maximum with increasing warfarin concentrations at different urea concentrations when excited at (A) 280nm and (B) 295nm. Different urea concentrations used were: 0.0 (●), 3.0 (○), 3.5 (▲), 4.0 (×), 4.5 (♦), 5.3 (◊), 6.5 (■), 8.0 (□) M.

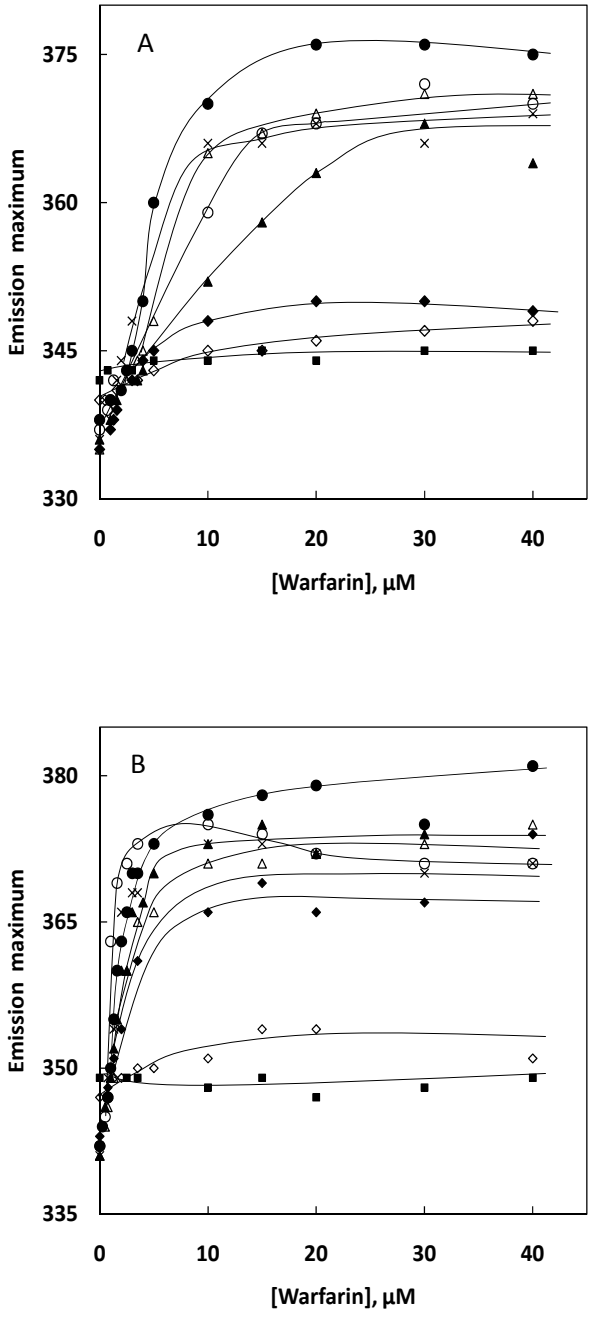

Figure 4.26 Plots showing change in the emission maximum of HSA with increasing warfarin concentrations at different urea concentrations when excited at (A) 280nm and (B) 295nm. Different urea concentrations used were: 0.0 (●), 3.0 (○), 3.5 (▲), 4.0 (Δ), 4.5 (×), 5.3 (♦), 6.5 (◊) and 8.0 (■) M.

drug concentrations. However, at higher urea concentrations, a linear decrease in the fluorescence intensity was noticed throughout the drug concentration range (Figure 4.25A). Plots of relative fluorescence intensity versus drug concentration obtained in presence of 3.0, 3.5 and 4.0M urea concentrations showed little variation, among each other but were found different from that obtained in the absence of urea. There was a progressive decrease in the fluorescence quenching with the increase in urea concentration at each drug concentration as the plots moved upwards on the Y-axis and became linear at higher urea concentrations (Figure 4.25A). Since the decrease in the fluorescence intensity (fluorescence quenching) with increasing warfarin concentrations was suggestive of warfarin binding to HSA, any decrease in the fluorescence quenching in presence of urea indicated loss in the drug binding to the protein. A significant loss in drug binding was noticed in presence of ≥6.5M urea due to lesser degree of quenching throughout the drug concentration range. At the highest drug concentration (40μM), about 39% and 31% quenching were noticed in presence of 6.5 and 8M urea respectively against 80% quenching observed with native HSA (Figure 4.25A). Similar conclusions can be drawn from Figure 4.40A where values of emission maximum have been plotted against warfarin concentration in presence of different concentrations of urea. The red shift became smaller at higher urea concentrations, indicating loss in drug binding to HSA.

To validate these findings, fluorescence spectra were also recorded under similar conditions but upon excitation at 295nm and the spectra are shown in Figures 4.27, 4.29, 4.31, 4.33, 4.35, 4.37 and 4.39. Both decrease in the fluorescence

intensity and significant red shift were noticed as shown in Figures 4.28, 4.30, 4.32, 4.34, 4.36, 4.38 and 4.40. Presence of urea in the incubation mixture caused both decrease in the fluorescence quenching as well as red shift in the emission maximum (Figures 4.25B and 4.26B). Although these results were found similar to those obtained with 280nm excitation, at lower drug concentrations, smaller differences were observed at higher drug concentrations (Figures 4.25 and 4.26). For example, at 40μM drug concentration, about 31% and 48% quenching in the fluorescence intensity were noticed in presence of 8M urea, when monitored upon excitation at 280 and 295nm respectively (Figure 4.25A and B). Similarly, a red shift of 15 and 24nm was observed at 30μM drug concentration in presence of 5.3M urea upon excitation at 280 and 295nm respectively (Figure 4.26A and B).

Presence of urea decreased the binding of warfarin to HSA as revealed by the decrease in fluorescence quenching and red shift in the emission maximum observed in the presence of urea (Figures 4.25 and 4.26). Drug binding data were analyzed in the same way as suggested by Eftink and Ghiron (1982). Stern-Volmer plots for warfarin-HSA interaction both in the absence and presence of different urea concentrations are shown in Figure 4.41. As can be seen from the figure, plots showed linearity at lower drug concentrations and significant deviation from linearity was noticed at higher drug concentrations. Values of the quenching constant (K_{sv}) as determined from the slope of initial linear parts of the plots are given in Table 4.1. A value of K_{sv} ($2.17\times 10^5\ \mathrm{M}^{-1}$) was obtained for warfarin-HSA interaction which was similar to those reported earlier for other drugs, known to bind site I of HSA (Wang *et al.,* 2011; Abdollahpour *et al.,* 2011)

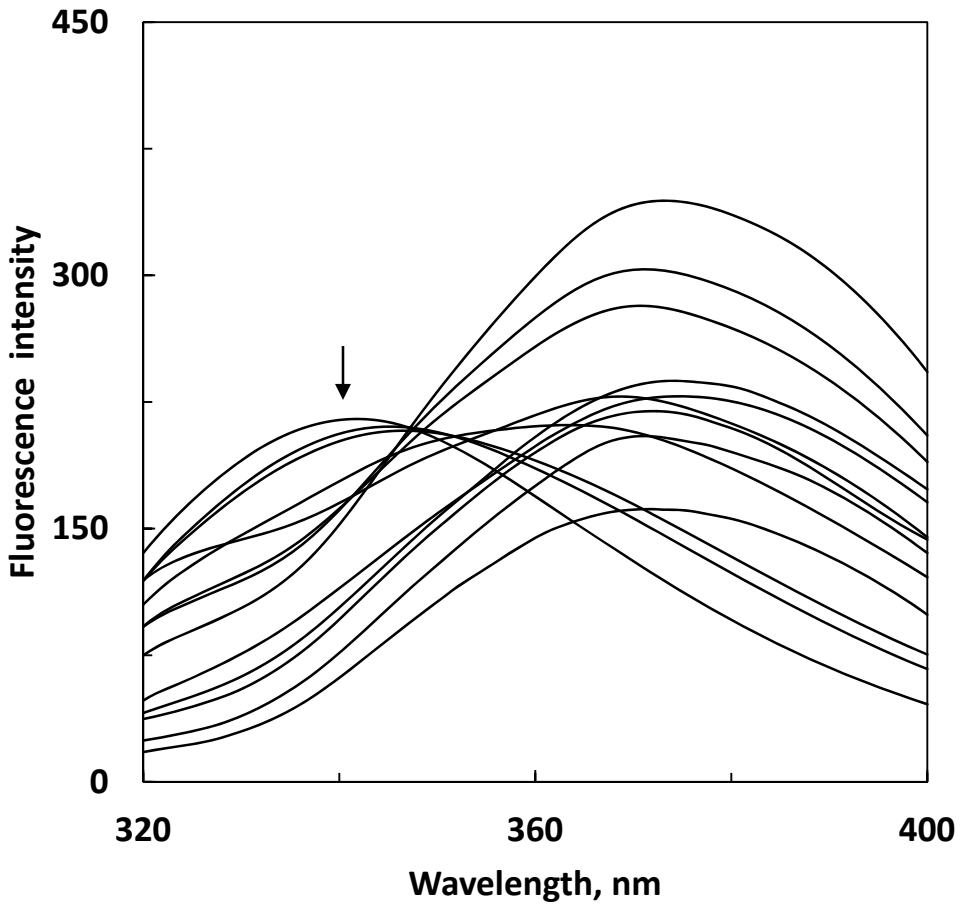

Figure 4.27 Fluorescence spectra of HSA (1.0μM) in the absence and presence of increasing warfarin concentrations but with 3.0M urea in 0.06M sodium phosphate buffer, pH 7.0 at 25℃ incubated for 60 minutes, upon excitation at 295nm. Warfarin concentrations from top to bottom (1-13) were: 0.0, 0.5, 0.75, 1.0, 1.6, 2.0, 2.5, 3.5, 10.0, 15.0, 20.0, 30.0 and 40.0μM respectively.

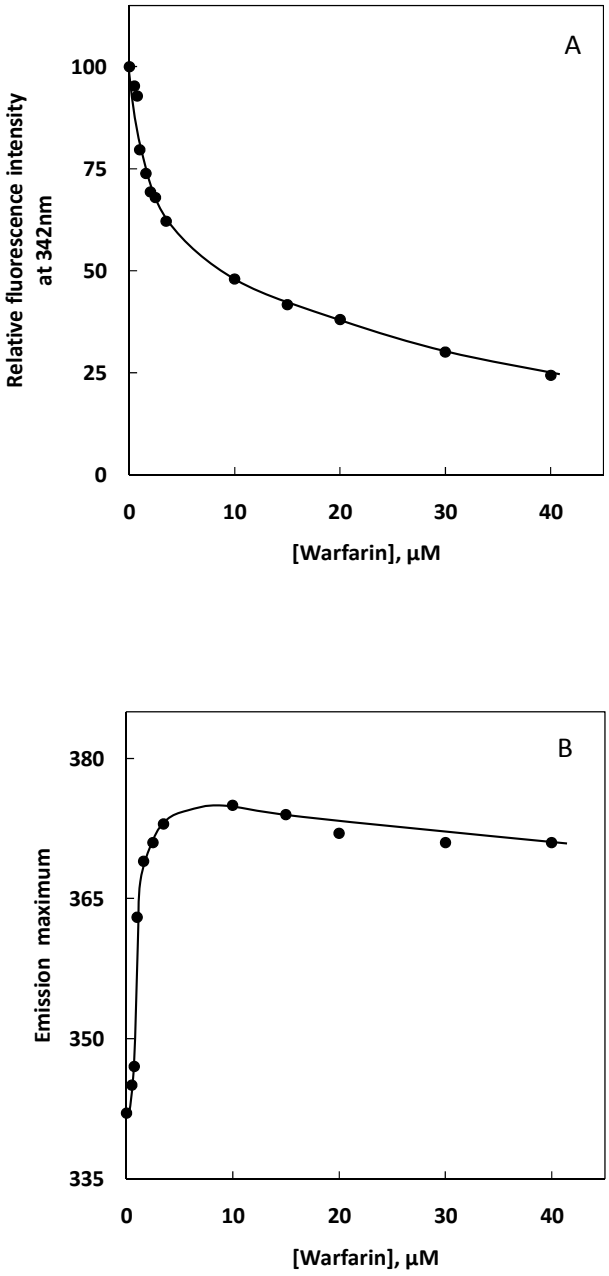

Figure 4.28 Plots showing change in the relative fluorescence intensity at 342nm upon excitation at 295nm (A) and the emission maximum (B) of HSA in 3.0M urea against warfarin concentration. Data of the relative fluorescence intensity and the emission maximum at different warfarin concentrations were obtained from Figure 4.27.

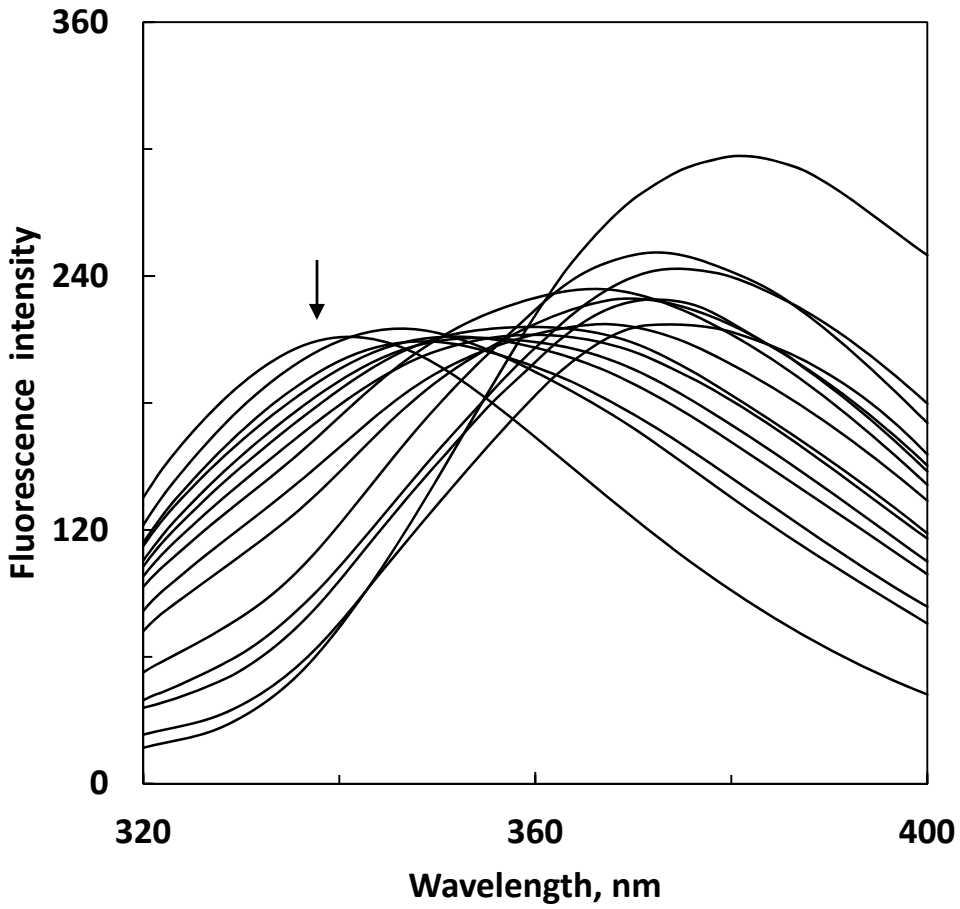

Figure 4.29 Fluorescence spectra of HSA (1.0μM) in the absence and presence of increasing warfarin concentrations but with 3.5M urea in 0.06M sodium phosphate buffer, pH 7.0 at 25℃ incubated for 60 minutes, upon excitation at 295nm. Warfarin concentrations from top to bottom (1-15) were: 0.0, 0.5, 1.0, 1.3, 1.6, 2.0, 2.5, 3.0, 4.0, 5.0, 10.0, 15.0, 20.0, 30.0 and 40.0μM respectively.

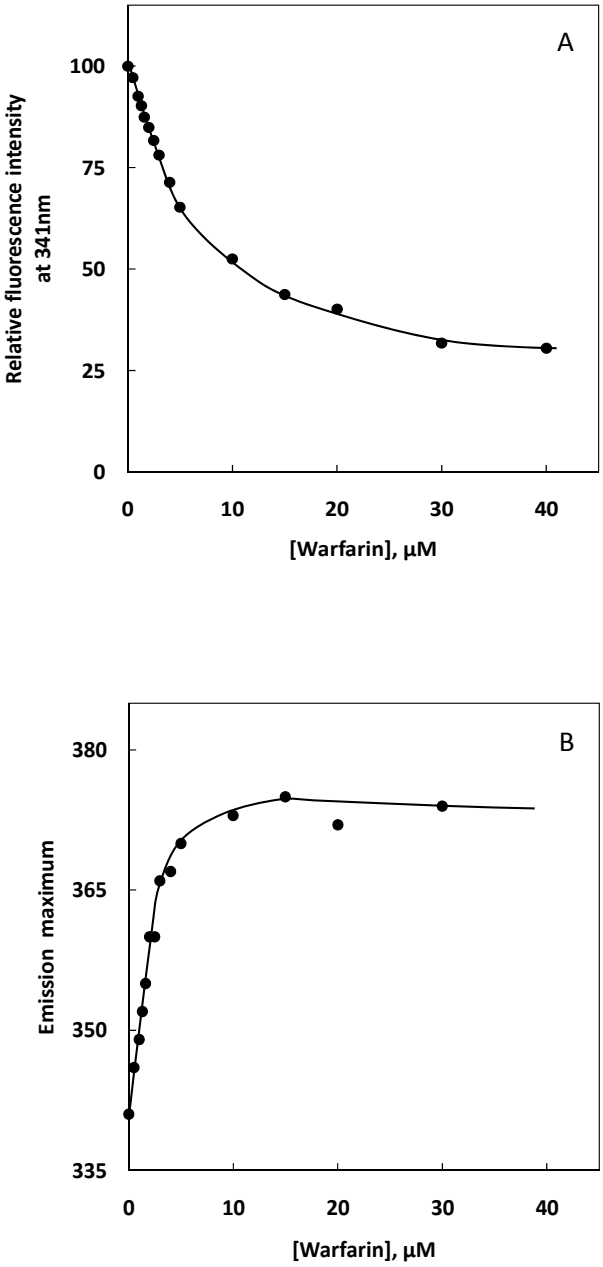

Figure 4.30 Plots showing change in the relative fluorescence intensity at 341nm upon excitation at 295nm (A) and the emission maximum (B) of HSA in 3.5M urea against warfarin concentration. Data of the relative fluorescence intensity and the emission maximum at different warfarin concentrations were obtained from Figure 4.29.

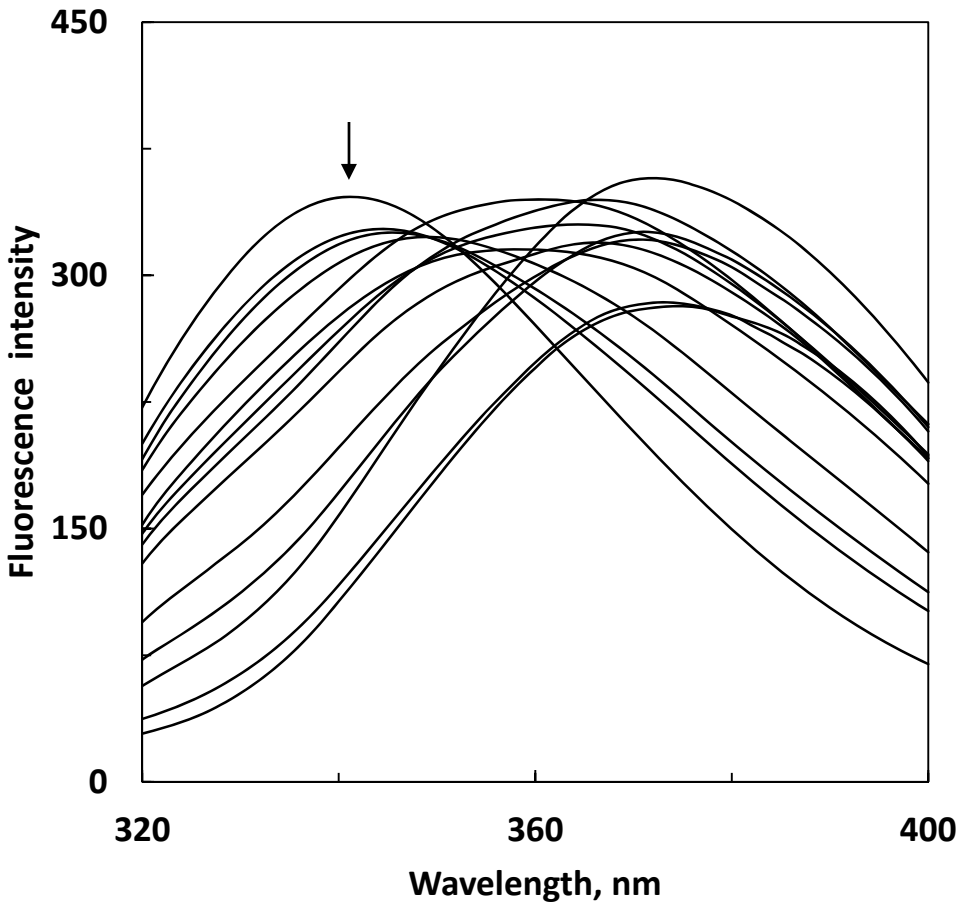

Figure 4.31 Fluorescence spectra of HSA (1.8μM) in the absence and presence of increasing warfarin concentrations but with 4.0M urea in 0.06M sodium phosphate buffer, pH 7.0 at 25℃ incubated for 60 minutes, upon excitation at 295nm. Warfarin concentrations from top to bottom (1-14) were: 0.0, 0.5, 0.75, 1.3, 2.5, 3.0, 3.5, 4.0, 5.0, 10.0, 15.0, 20.0, 30.0 and 40.0μM respectively.

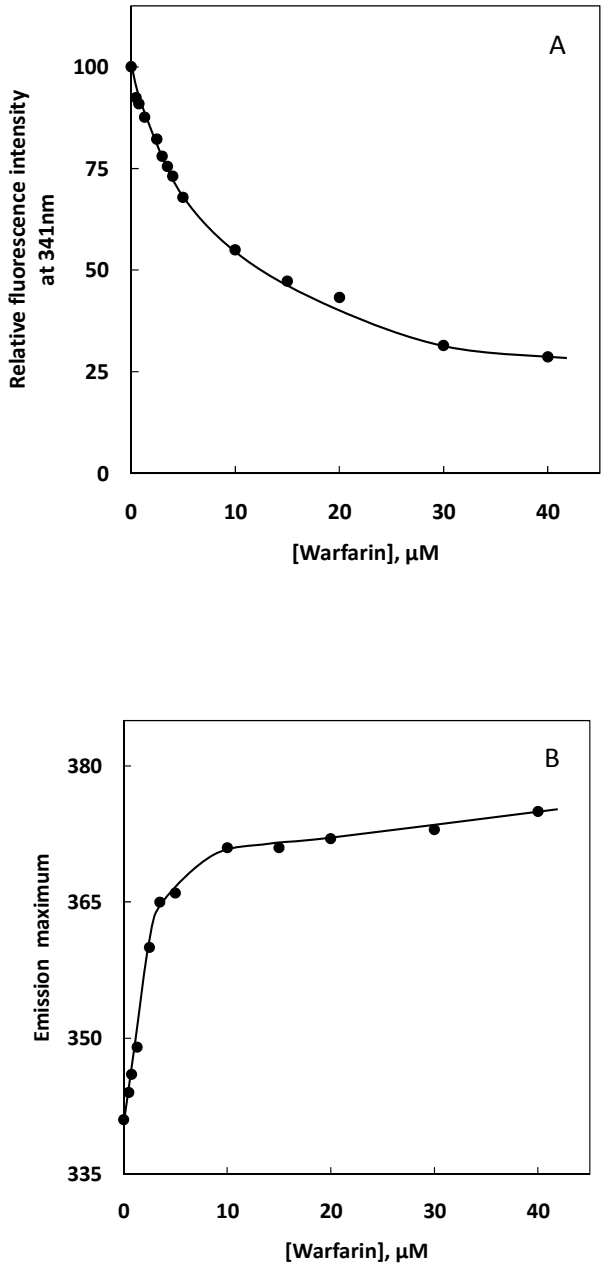

Figure 4.32 Plots showing change in the relative fluorescence intensity at 341nm upon excitation at 295nm (A) and the emission maximum (B) of HSA in 4.0M urea against warfarin concentration. Data of the relative fluorescence intensity and the emission maximum at different warfarin concentrations were obtained from Figure 4.31.

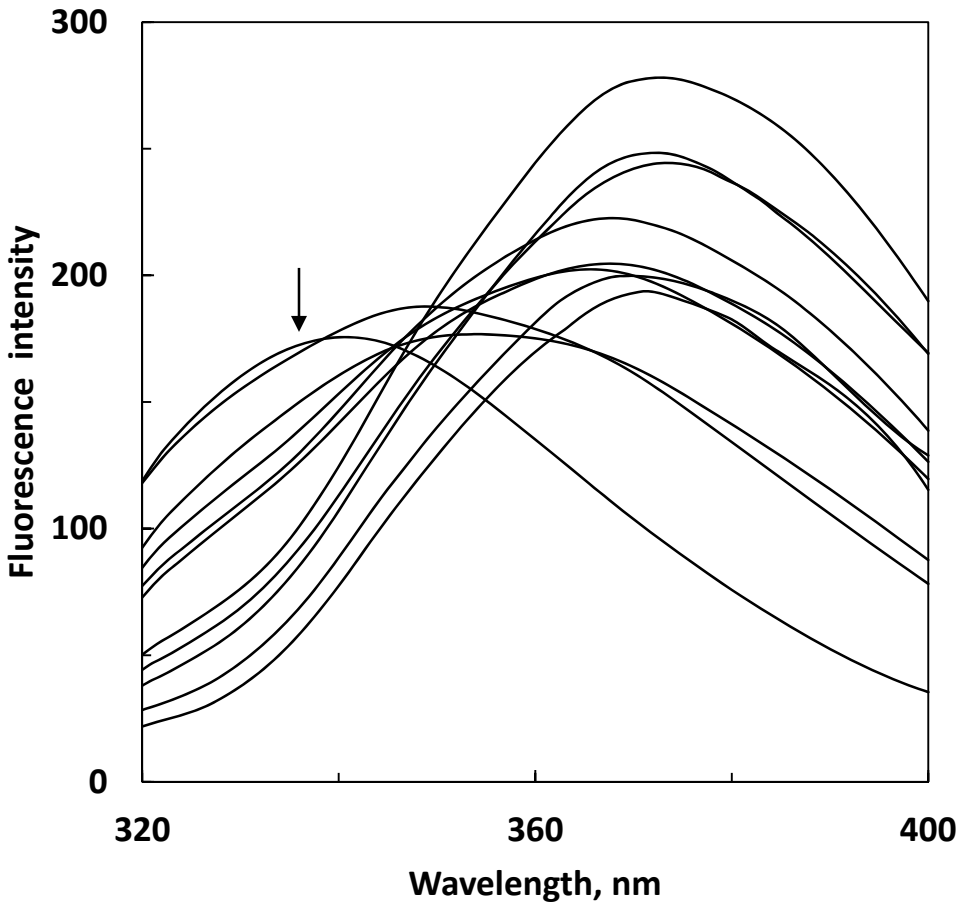

Figure 4.33 Fluorescence spectra of HSA (1.0μM) in the absence and presence of increasing warfarin concentrations but with 4.5M urea in 0.06M sodium phosphate buffer, pH 7.0 at 25℃ incubated for 60 minutes, upon excitation at 295nm. Warfarin concentrations from top to bottom (1-11) were: 0.0, 0.75, 1.3, 2.0, 3.0, 3.5, 10.0, 15.0, 20.0, 30.0 and 40.0μM respectively.

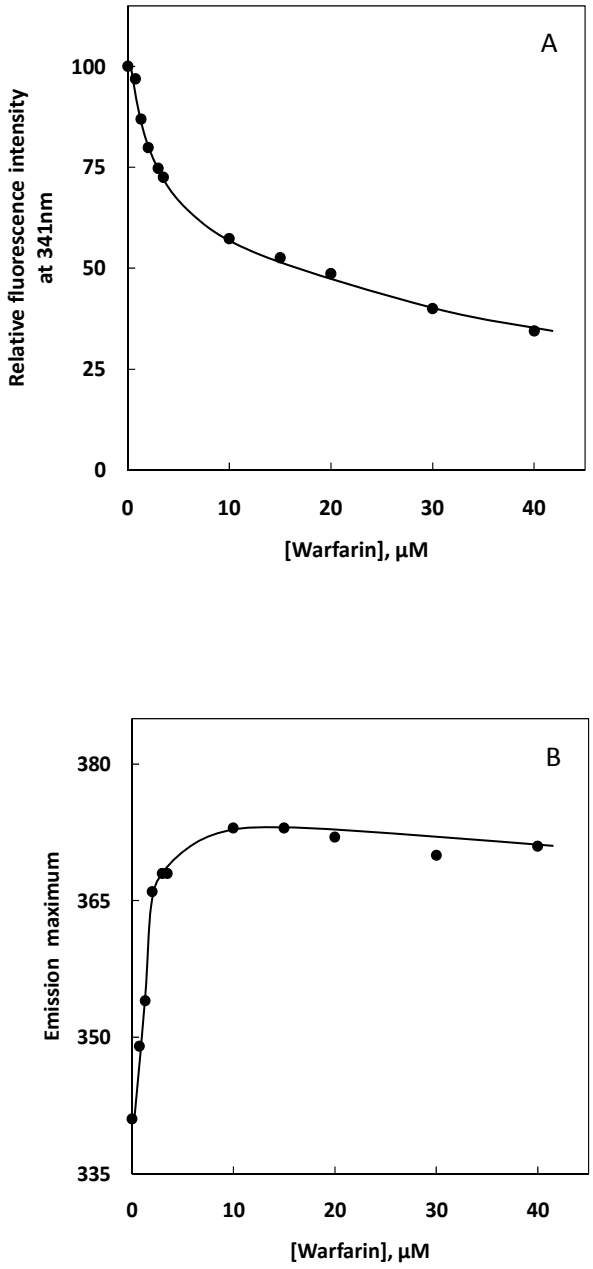

Figure 4.34 Plots showing change in the relative fluorescence intensity at 341nm upon excitation at 295nm (A) and the emission maximum (B) of HSA in 4.5M urea against warfarin concentration. Data of the relative fluorescence intensity and the emission maximum at different warfarin concentrations were obtained from Figure 4.33.

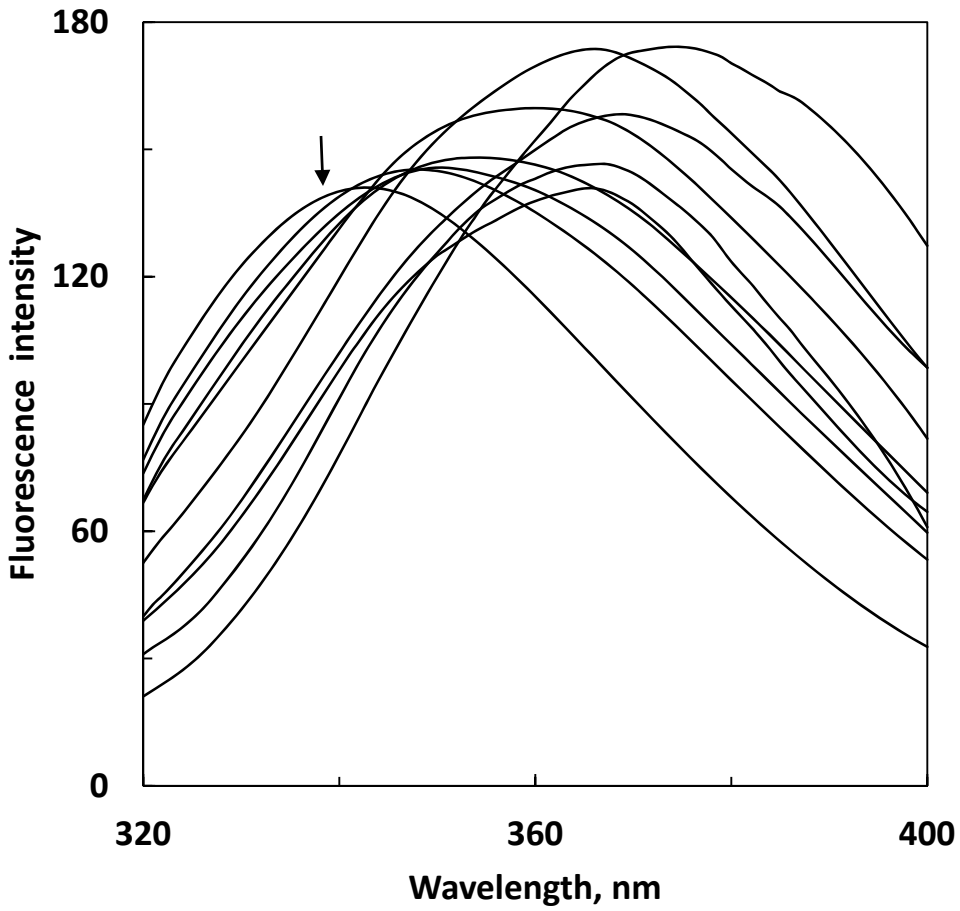

Figure 4.35 Fluorescence spectra of HSA (1.0μM) in the absence and presence of increasing warfarin concentrations but with 5.3M urea in 0.06M sodium phosphate buffer, pH 7.0 at 25℃ incubated for 60 minutes, upon excitation at 295nm. Warfarin concentrations from top to bottom (1-10) were: 0.0, 0.75, 1.3, 2.0, 3.5, 10.0, 15.0, 20.0, 30.0 and 40.0μM respectively.

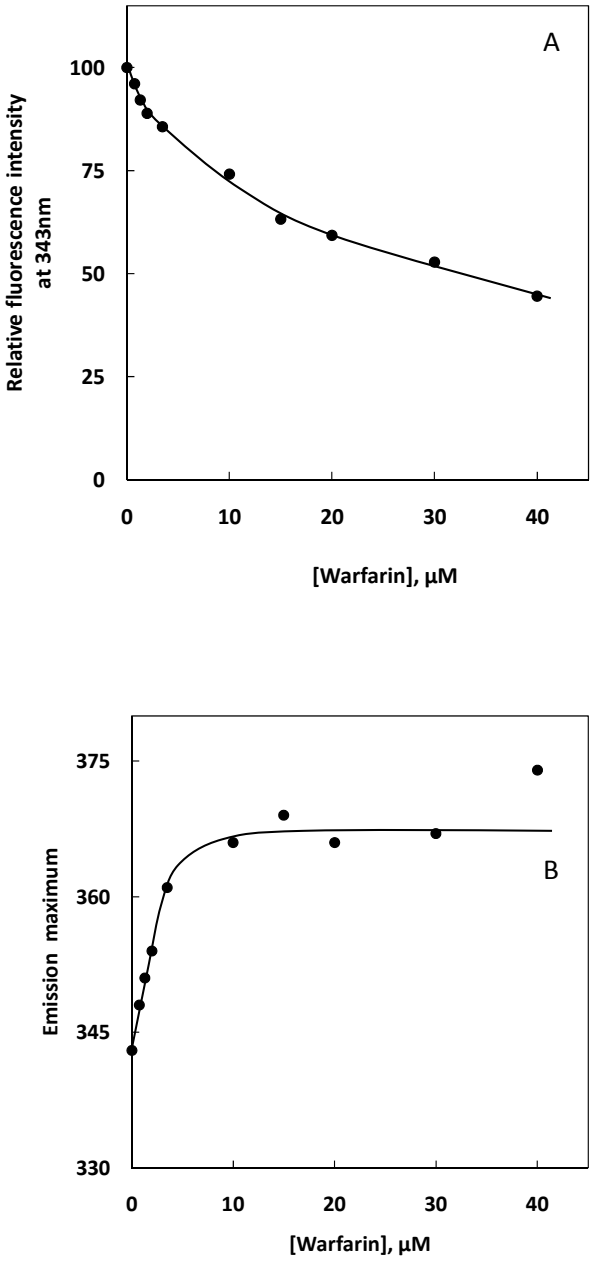

Figure 4.36 Plots showing change in the relative fluorescence intensity at 343nm upon excitation at 295nm (A) and the emission maximum (B) of HSA in 5.3M urea against warfarin concentration. Data of the relative fluorescence intensity and the emission maximum at different warfarin concentrations were obtained from Figure 4.35.

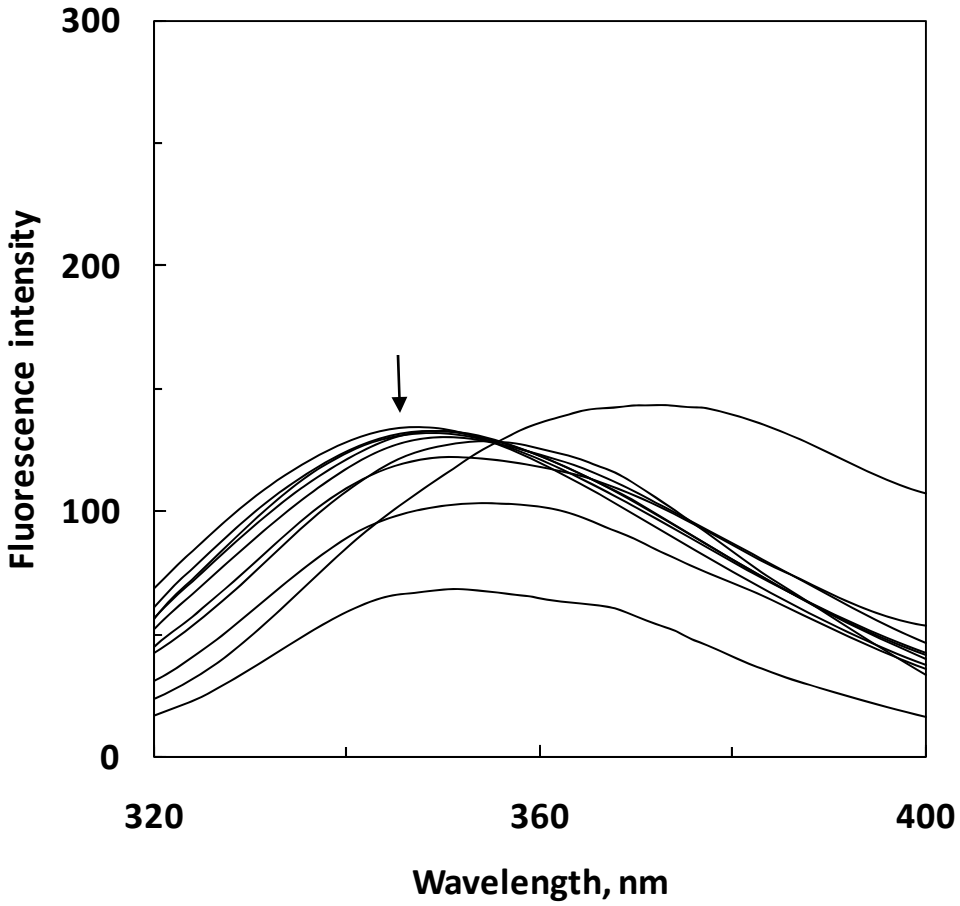

Figure 4.37 Fluorescence spectra of HSA (1.0μM) in the absence and presence of increasing warfarin concentrations but with 6.5M urea in 0.06M sodium phosphate buffer, pH 7.0 at 25℃ incubated for 60 minutes, upon excitation at 295nm. Warfarin concentrations from top to bottom (1-10) were: 0.0, 1.3, 2.0, 3.5, 5.0, 10.0, 15.0, 20.0, 30.0 and 40.0μM respectively.

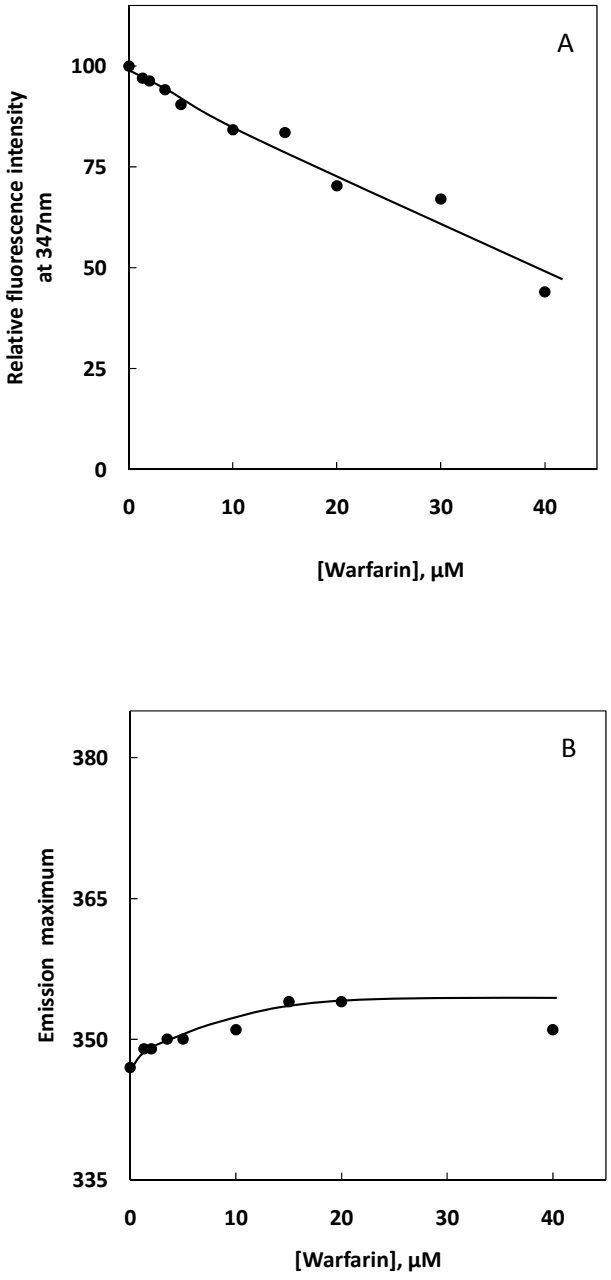

Figure 4.38 Plots showing change in the relative fluorescence intensity at 347nm upon excitation at 295nm (A) and the emission maximum (B) of HSA in 6.5M urea against warfarin concentration. Data of the relative fluorescence intensity and emission maximum at different warfarin concentrations were obtained from Figure 4.37.

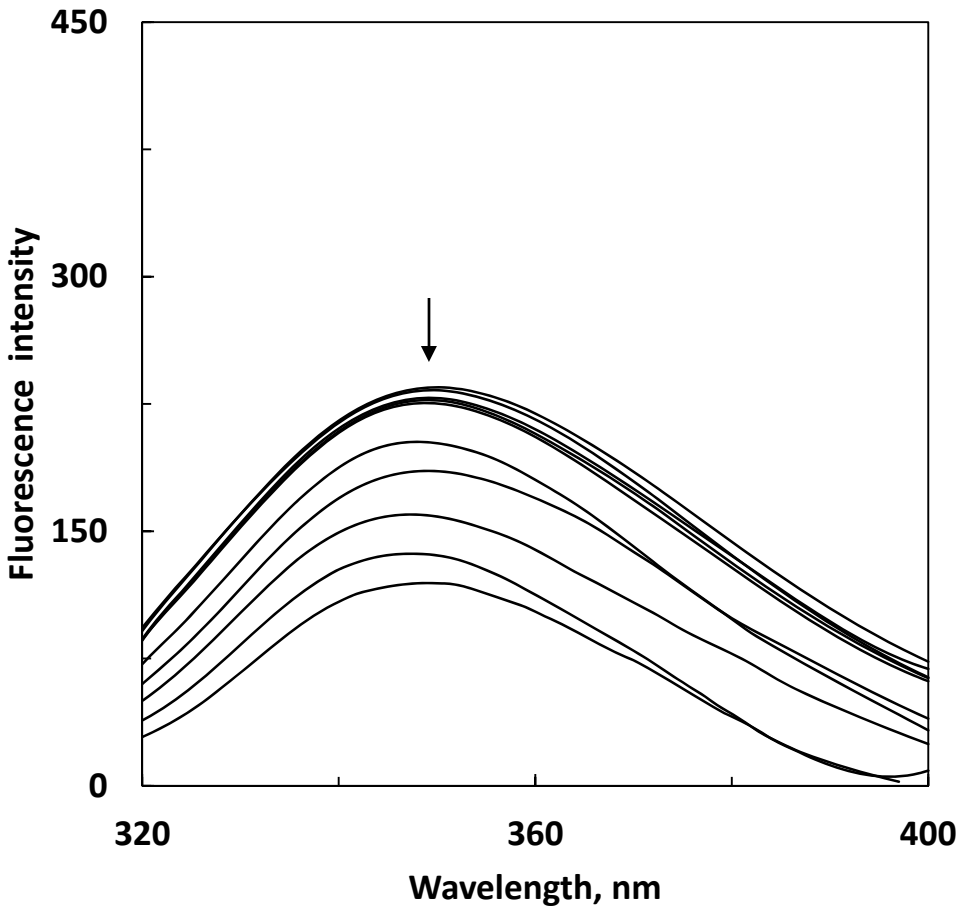

Figure 4.39 Fluorescence spectra of HSA (1.8μM) in the absence and presence of increasing warfarin concentrations but with 8.0M urea in 0.06M sodium phosphate buffer, pH 7.0 at 25℃ incubated for 60 minutes, upon excitation at 295nm. Warfarin concentrations from top to bottom (1-10) were: 0.0, 1.0, 2.5, 3.0, 3.5, 10.0, 15.0, 20.0, 30.0 and 40.0μM respectively.

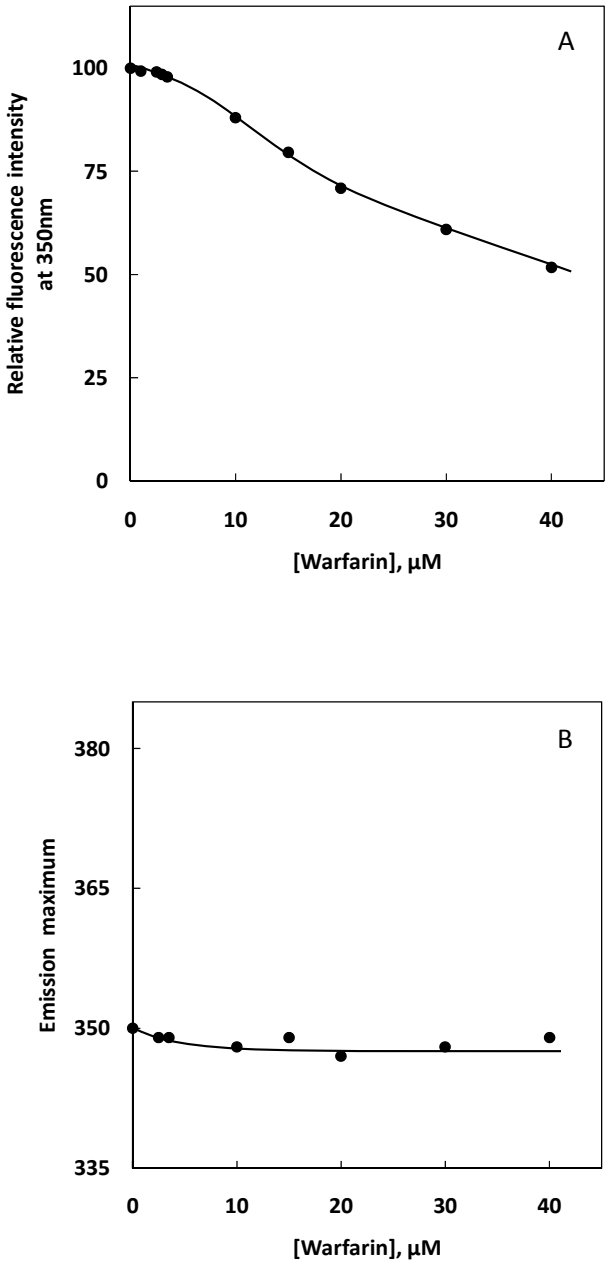

Figure 4.40 Plots showing change in the relative fluorescence intensity at 350nm upon excitation at 295nm (A) and the emission maximum (B) of HSA in 8.0M urea against warfarin concentration. Data of the relative fluorescence intensity and the emission maximum at different warfarin concentrations were obtained from Figure 4.39.

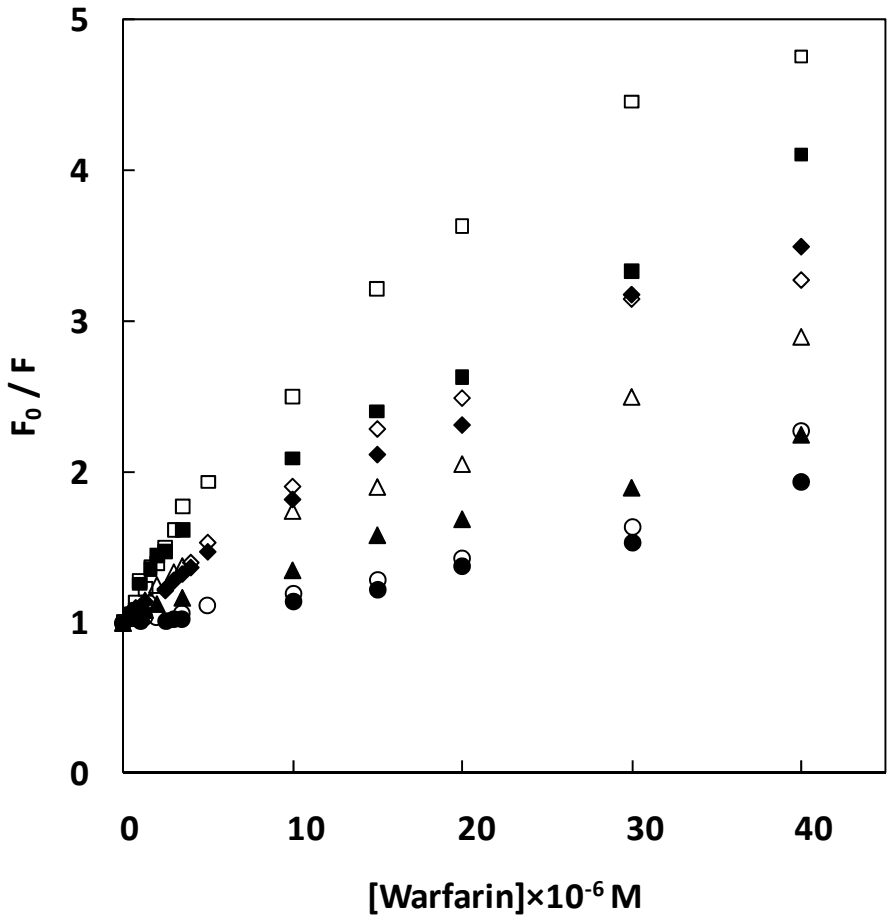

Figure 4.41 Stern-Volmer plots for tryptophan fluorescence quenching of HSA at increasing warfarin concentrations in the absence and presence of different urea concentrations; 0.0 (□), 3.0 (■), 3.5 (◊), 4.0 (♦), 4.5 (Δ), 5.3 (▲), 6.5 (○) and 8.0 (●) M urea.

Table 4.1 Values of the Stern-Volmer constant (Ksv) for tryptophan fluorescence quenching of HSA upon warfarin binding in the absence and presence of different urea concentrations.

[Urea] M	$\boldsymbol{K_{sv}}$ $[\mathbf{M^{-1}}]$	$\boldsymbol{R^2}$
0.0	2.17×10^5	0.992
3.0	1.39×10^5	0.9982
3.5	1.06×10^5	0.9917
4.0	9.03×10^4	0.993
4.5	1.09×10^5	0.9908
5.3	6.39×10^4	0.9956
6.5	1.88×10^4	0.9929
8.0	5.34×10^3	0.8828

$R^2 =$ Correlation coefficient

There was a significant decrease in K_{sv} value with increasing urea concentrations. Decrease in the K_{sv} value with increasing urea concentrations suggested the increase in the distance between excited fluorophore (Trp) and the ligand (warfarin). Therefore the tertiary structure of the protein was destabilized at higher urea concentrations.

Apparent binding constant, K_b for warfarin-HSA interaction were determined from the plots shown in Figure 4.42 and the values of K_b are listed in Table 4.2. Value of binding constant, $2.1\times 10^5\ \mathrm{M}^{-1}$ as obtained in this study was similar to the one reported earlier (Wilting *et al.,* 1980; Fleury *et al.,* 1997). The binding constant decreased from $2.1\times\ 10^5\ \mathrm{M}^{-1}$ under native conditions to $4.7\times\ 10^3\ \mathrm{M}^{-1}$ in the presence of 5.3M urea. Although, there was a decrease in both Stern-Volmer constant (K_{sv}) and apparent binding constant (K_b) with increasing urea concentrations, it was more pronounced in K_b at higher urea concentrations (e.g. 5.3M). These results suggested the sensitivity of warfarin binding site to urea as alteration in the three-dimensional structure of HSA markedly affected its drug binding ability.

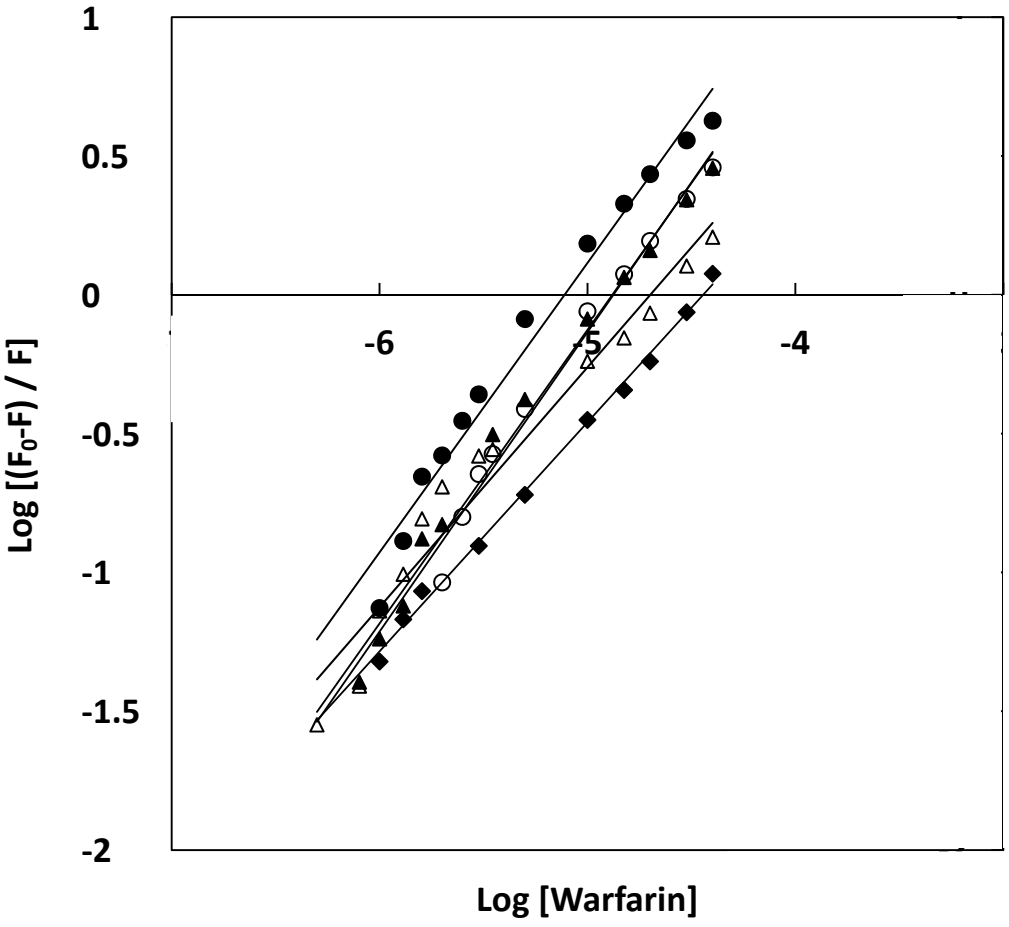

Figure 4.42 Plots of Log [(F0-F)/ F] versus Log [Warfarin] in the absence and presence of different urea concentrations. Values of F_0 and F were taken from Figure 4.25 A. Different urea concentrations used were: 0.0 (●), 3.5 (○), 4.0 (▲), 4.5 (Δ) and 5.3 (♦) M urea.

Table 4.2 Values of the binding constant (K_b) for the warfarin-HSA complex in the absence and presence of different urea concentrations.

[Urea] M	$\mathbf{K_b[M^{-1}]}$	$\mathbf{R^2}$
0.0	2.1×10^5	0.9755
3.5	1.7×10^5	0.9832
4.0	1.4×10^5	0.9864
4.5	1.1×10^4	0.959
5.3	4.7×10^3	0.9962

$R^2 =$ Correlation coefficient